Copernicus Sentinel-3 Surface Topography Mission - Cyclic Performance Report

LAND ICE

S3A Cycle No. 102 Start date: 03/08/2023 End date: 30/08/2023	S3B Cycle No. 083 Start date: 13/08/2023 End date: 09/09/2023

Reference: S3MPC-STM_CPR_0007-102-083

Issue 1.0 – 21/08/2023

Contract: 4000136824/21/I-BG

CHRONOLOGY ISSUES

Issue	Date	Object	Written by	Checked by	Approved by
1.0	14/09/2023	Creation	DTU Space	J. Aublanc	G. Jettou

ACCEPTANCE

	CLIENT: ESA	SUPPLIER: CLS
Name	Pierre Féménias	Ghita Jettou
Function	ESA Technical Officer	MPC Service Manager

LIST OF CONTENTS

LIST OF TABLES

LIST OF FIGURES

1 Introduction

The purpose of this document is to report on the performance and data quality of the Copernicus Sentinel-3 Surface Topography Mission (STM) LAND products. The constellation currently includes Sentinel-3A and Sentinel-3B altimetry satellites. This document is associated with data dissemination on a cyclic basis and is generated a few days after the end of Sentinel-3B cycle.

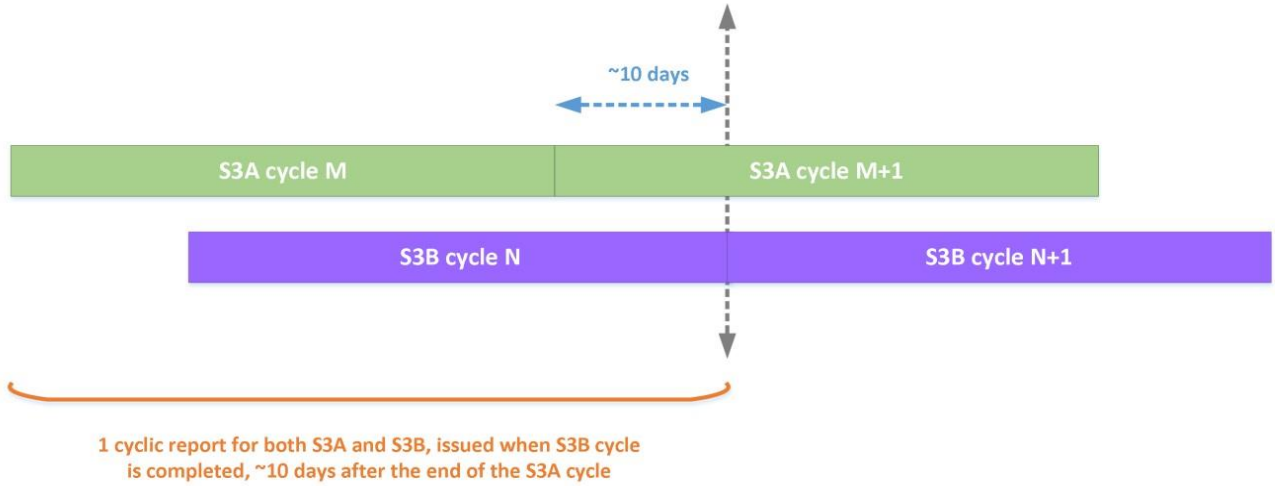

Figure 1: S3A and S3B cycles chronology

The SRAL Level 2 products assessed hereafter are produced by the ESA Sentinel-3 LAND Processing Centre. One of the main goals of the cyclic report is to detect and report as quickly as possible any events, or anomaly, impacting the data quality. Subsequently, the assessments are made on the Short Time Critical (STC) products, generally delivered 48 hours after data acquisitions. Differences are expected with the Non Time Critical (NTC) products, for which the orbit data and several geophysical corrections are consolidated.

The main objectives of this document are:

- To provide a data quality assessment of the Sentinel-3 SRAL Level 2 STC LAND products
- To report on any changes likely to impact data quality at any level, from instrument status to software configuration.
- To present the major useful results for S3A cycle 102, from 03/08/2023 to 30/08/2023.
- To present the major useful results for S3B cycle 083, from 13/08/2023 to 09/09/2023.

2 Cycle overview

During these cycles, Sentinel-3A and Sentinel-3B SRAL operated in SAR mode over the ice sheets. For Level-2 STC Land ice products over the polar ice sheets the OCOG (Ice-1) retracker provides the largest amount of ice sheet elevation data, and most failures are located close to the ice sheet margins.

Parameter:	Sentinel-3A	Sentinel-3B
Orbit	Nominal	There are duplicated orbit files. See Section 4.1.
Availability of geophysical corrections	A few ocean tide measurements are missing over the Antarctic Ice Shelves. See Table 4.2 - 4.4. This is assumed as nominal.	A few ocean tides measurements are missing over the Antarctic Ice Shelves. See Table 4.2 - 4.4. This is assumed as nominal.
Availability of auxiliary data	Nominal auxiliary data availability	Nominal auxiliary data availability
Geophysical parameters	Nominal	Nominal
Specific investigations	N/A	N/A
Orbit cross-over statistics	The UCL ice sheet retracker enables fewer cross-overs to be evaluated than for the OCOG/ICE-1 retracker. The ratio between the number of cross-overs for the two retracker is normal. For cross-overs less than 1 meter shows a median bias less than 2.6 centimetre and a standard deviation less than 36 cm.	The UCL ice sheet retracker enables fewer cross-overs to be evaluated than for the OCOG/ICE-1 retracker. The ratio between the number of cross-overs for the two retracker is normal. For cross-overs less than 1 meter shows a median bias less than one centimetre and a standard deviation < 36 cm.
Status	See Specific investigation	See Specific investigation

Table 2.1 General overview of the data availability and mission performances for the S3A and S3B cycles evaluated Colours indicate performance: OK (green), Warning (yellow), and Not ok (red)

Color legend:

(green)	OK
(yellow)	Warning
(red)	Not OK

3 Processing baseline

Table 2 details the versions of the Processing Baseline (PB), and Level-1 and Level-2 Instrument Processing Facility software used for the products assessed. This is part of the Baseline Collection (BC) 004.

Cycle		Processing Baseline	IPF SM2 version	IPF SR1 version	IPF MW1 version
Sentinel-3A	102	3.05	06.20	06.20	06.13
Sentinel-3B	083	3.05			

Table 2: Processing baseline and IPF details

The evolutions of the Sentinel-3 STM Processing Baseline since July 2016, end of commissioning phase, are summarized in the "Sentinel Online" Web pages:
https://sentinels.copernicus.eu/web/sentinel/technical-guides/sentinel-3-altimetry/processing-baseline

Sentinel-3 Land Altimetry Thematic Products (Baseline Collection 005) will replace the present product. See the transfer to operation plan at: https://sentinels.copernicus.eu/web/sentinel/-/sentinel-3-land-altimetry-land-thematic-products-with-baseline-collection-005-availability-notice-update-on-28-march-2023?redirect=%2Fweb%2Fsentinel%2Fhome

4 Data availability and missing measurements

4.1 Orbit coverage and missing measurements

There may occur delays in the processing of the data at the processing centre, which means that the data products assessed in the cyclic reports might not represent 100% of the orbits in the full cycle. The percentage of L2 products of the full cycle, which this report builds on is presented in Table 4.1.

It is expected that there will be one file generated per pass, and two passes per orbit. Therefore, it can be anticipated that a total of 770 files will be received. For S3A all files are received. For S3B, 774 files are received out of 770 expected, this is due to a split/duplication of files for orbits 022, 137, 278. There are no missing passes.

Table 4.1 Data availability and the percentage of the full cycle of STC products

Cycle		Product type	Latency	Passes	Expected passes	% passes received
Sentinel-3A	102	SR_2_LAN	STC	770	770	100%
Sentinel-3B	083			770	770	100%

4.2 Modes of operations

The on-board tracker of the Sentinel-3 altimeter has three different possible modes:

- **Closed-loop mode**: autonomous positioning of the range window using the median algorithm
- **Open-loop mode:** range window position based on a priori knowledge of terrain altitude derived from a Digital Elevation Model (DEM).
- **Open-loop with fixed gain mode in addition to open-loop, constant acquisition gain values are applied**

Figure 4.1 shows the tracking modes for both S3A and S3B. Mainly, the acquisition of the satellites is in closed-loop, except for Elephant Island and Coronation Island in the Southern Ocean where the tracking modes are Open-loop. In addition, open-loop commands have been defined for S3A over several specific continental glaciers (for glaciers in Himalaya, Patagonia, Alpes, Pyrénées, Andes, Tadjikistan and Victoria Land in Antarctica).

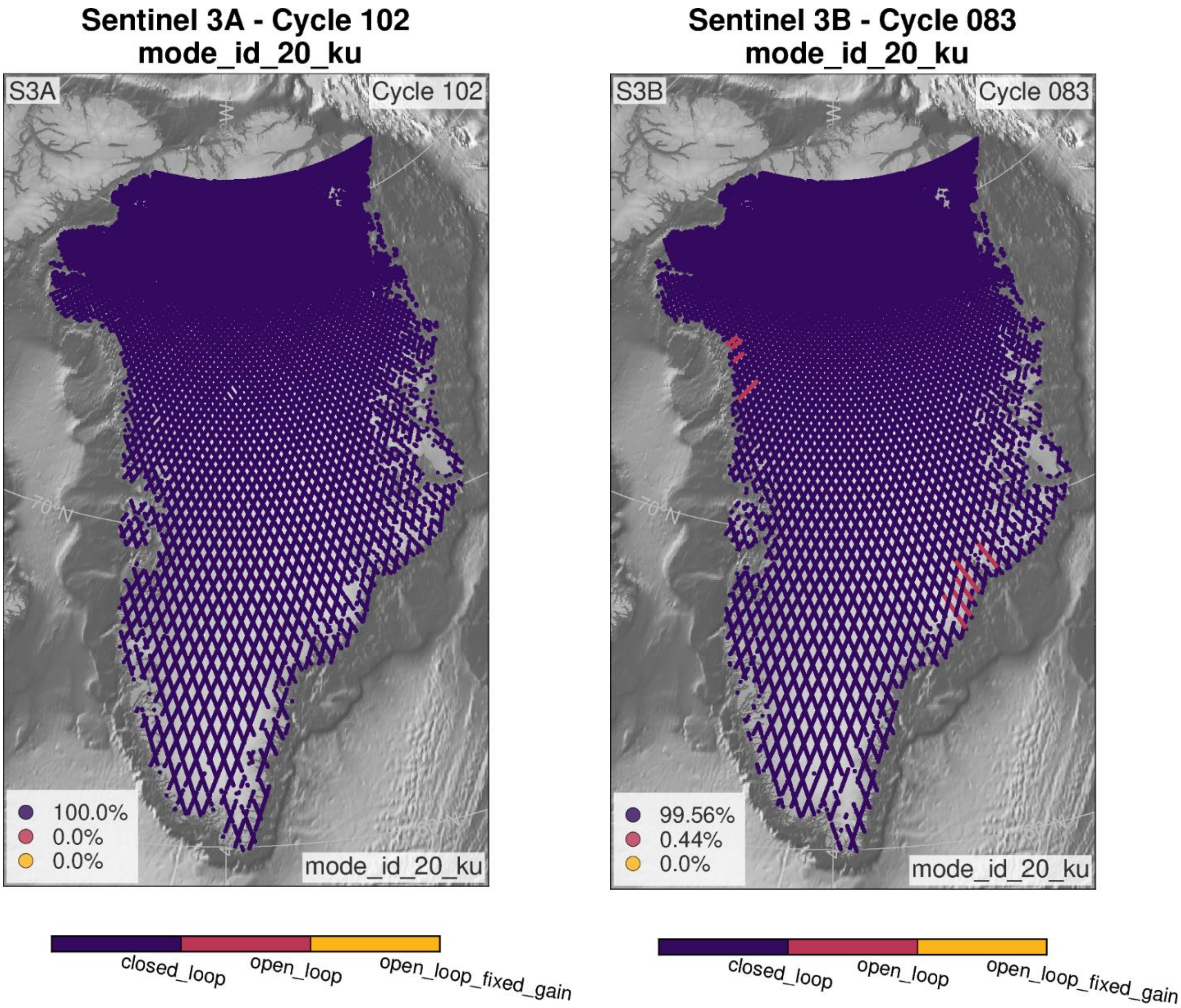

Figure 4.1 Tracking mode for S3A and S3B over Greenland from the mode_id_20_ku parameter

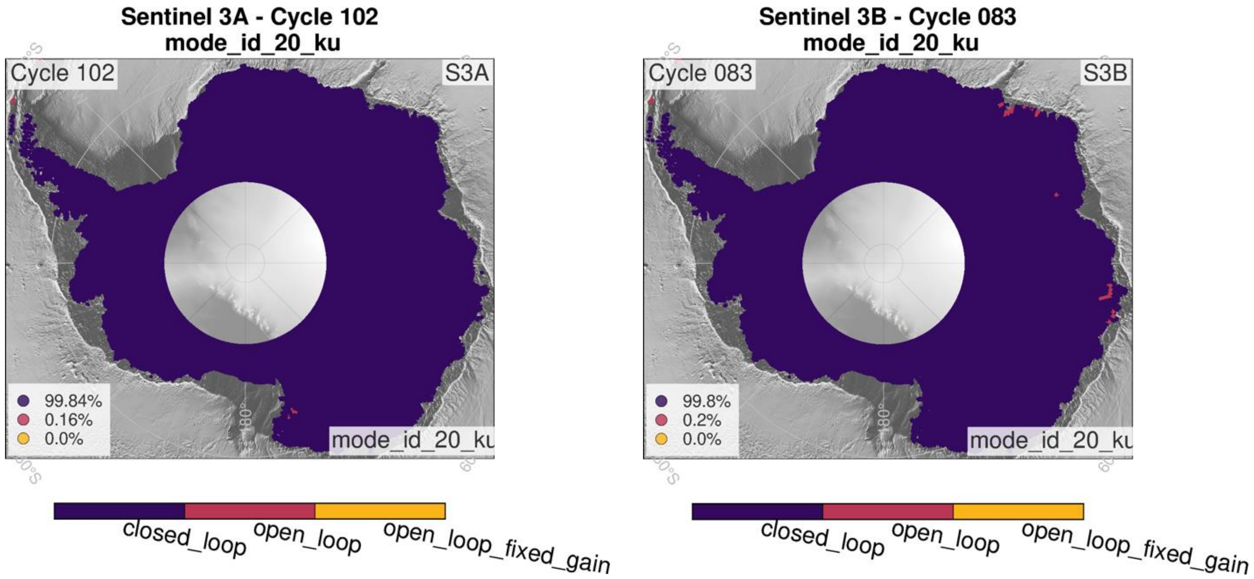

Figure 4.2 Tracking mode for S3A and S3B over Antarctica from the mode_id_20_ku parameter

Since October 24th, 2023, new Open Loop Tracking Commands were uploaded on **Sentinel-3B** for 50 track portions over land ice. The Figure below shows the location of these track portions, located over the Antarctica and Greenland ice sheet margins, Svalbard (Austfonna glacier), Iceland (Vatnajökull glacier). There was also an update of OTLC for two track portions in Karakoram (Himalayas). The objectives are to test a new methodology in the OLTC definition over land ice, and to assess the benefits compared to closed-loop tracking mode in terms of data coverage and SNR.

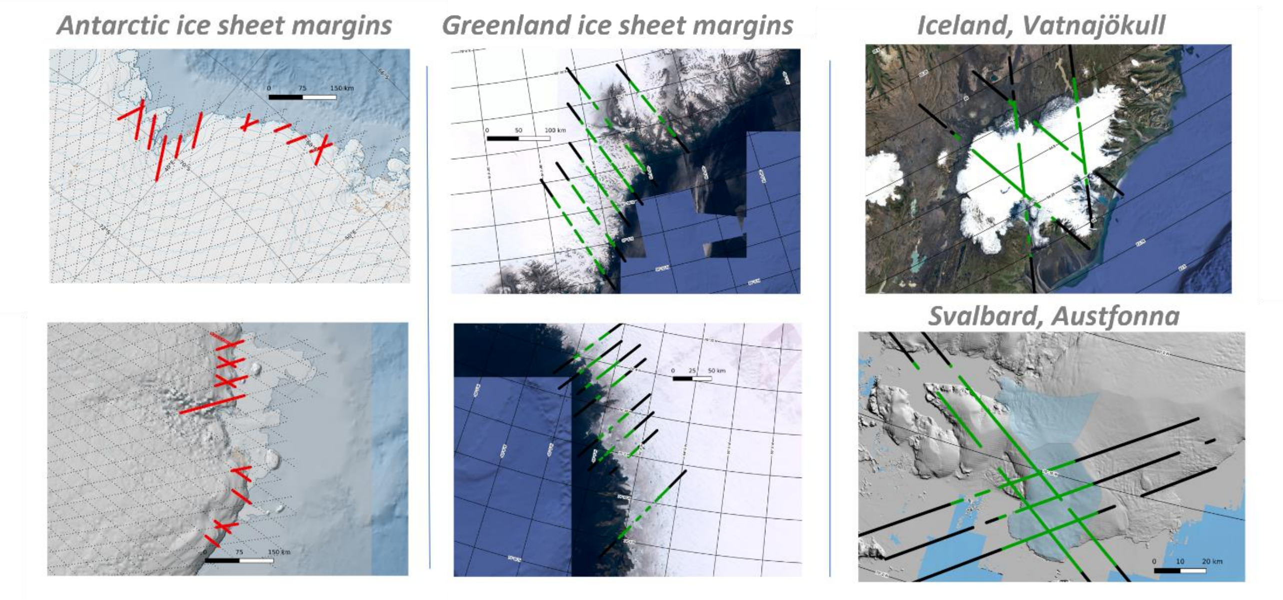

Figure 4.3 Locations of the 50 track portions for which new OLTC were uploaded on-board Sentinel-3B on October 24th 2023 (red colour in Antarctica, green colour over Greenland, Iceland and Svalbard)

4.3 Availability of geophysical corrections

The range from the satellite to the surface for each measurement is computed by applying several geophysical corrections and internal delay to the initial uncorrected range. It is important to track the availability and validity of these corrections since they are required for the final L2 elevation parameters and the derived ice sheet surface elevation change. The data over ice sheets and ice shelves are selected by using the *surface_class* flag (Section 4.4.2) over Greenland and Antarctica.

In this section the availability of geophysical corrections in the L2 products over ice sheets and ice shelves are analysed and presented.

4.3.1 Availability of Geophysical Corrections over Ice Sheets

The geophysical corrections usually relevant for range measurements over ice sheets are the dry and wet troposphere, ionosphere delays, solid Earth tide, ocean loading tide, and polar tide. Table 4.2 and Table 4.3 summarize the availability for the Greenland and Antarctica Ice Sheets, for S3A and S3B.

S3A

Geophysical Correction	Availability (%)
iono_cor_gim_01_ku	100.00
load_tide_sol1_01	100.00
load_tide_sol2_01	100.00
mod_dry_tropo_cor_meas_altitude_01	100.00
mod_wet_tropo_cor_meas_altitude_01	100.00
ocean_tide_non_eq_01	100.00
pole_tide_01	100.00
solid_earth_tide_01	100.00

S3B

Geophysical Correction	Availability (%)
iono_cor_gim_01_ku	100.00
load_tide_sol1_01	100.00
load_tide_sol2_01	100.00
mod_dry_tropo_cor_meas_altitude_01	100.00
mod_wet_tropo_cor_meas_altitude_01	100.00
ocean_tide_non_eq_01	100.00
pole_tide_01	100.00
solid_earth_tide_01	100.00

Table 4.2 Percentage of Geophysical Correction availability over the Greenland ice sheet

S3A

Geophysical Correction	Availability (%)
iono_cor_gim_01_ku	100.00
load_tide_sol1_01	100.00
load_tide_sol2_01	100.00
mod_dry_tropo_cor_meas_altitude_01	100.00
mod_wet_tropo_cor_meas_altitude_01	100.00
ocean_tide_non_eq_01	100.00
pole_tide_01	100.00
solid_earth_tide_01	100.00

S3B

Geophysical Correction	Availability (%)
iono_cor_gim_01_ku	100.00
load_tide_sol1_01	100.00
load_tide_sol2_01	100.00
mod_dry_tropo_cor_meas_altitude_01	100.00
mod_wet_tropo_cor_meas_altitude_01	100.00
ocean_tide_non_eq_01	100.00
pole_tide_01	100.00
solid_earth_tide_01	100.00

Table 4.3 Percentage of Geophysical Correction availability over the Antarctic Ice Sheet

4.3.2 Availability of Geophysical Corrections over Ice Shelves

Over the Antarctic ice shelves, the usual corrections applied to the range are the same as for the ice sheets including ocean tide and inverse barometric corrections. Table 4.4 summarizes the availability for S3A and S3B.

Geophysical Correction (S3A)	Availability (%)
hf_fluct_cor_01	100.00
inv_bar_cor_01	100.00
iono_cor_gim_01_ku	100.00
load_tide_sol1_01	100.00
load_tide_sol2_01	100.00
mod_dry_tropo_cor_meas_altitude_01	100.00
mod_wet_tropo_cor_meas_altitude_01	100.00
ocean_tide_non_eq_01	100.00
ocean_tide_sol1_01	98.83
ocean_tide_sol2_01	99.53
pole_tide_01	100.00
solid_earth_tide_01	100.00

Geophysical Correction (S3B)	Availability (%)
hf_fluct_cor_01	100.00
inv_bar_cor_01	100.00
iono_cor_gim_01_ku	100.00
load_tide_sol1_01	100.00
load_tide_sol2_01	100.00
mod_dry_tropo_cor_meas_altitude_01	100.00
mod_wet_tropo_cor_meas_altitude_01	100.00
ocean_tide_non_eq_01	100.00
ocean_tide_sol1_01	98.84
ocean_tide_sol2_01	99.53
pole_tide_01	100.00
solid_earth_tide_01	100.00

Table 4.4 Percentage of Geophysical Correction availability over the Antarctic Ice Shelves.

4.4 Availability of auxiliary data

The S3A and S3B products contain several geophysical parameters, which are derived from auxiliary data, and which are useful for the end-user of the data products. These parameters include surface type, surface class, and slope correction. In the following, these geophysical parameters for the current S3A and S3B cycles are presented.

4.4.1 20 Hz Ku Band Surface Type (surf_type_20_ku)

The 20 Hz Ku band surface type parameter (surf_type_20_ku) is derived from a static grid which provides four types: open oceans or semi-enclosed seas, enclosed seas or lakes, continental ice, and land. The surf_class_20_ku parameter for the current cycles of S3A and S3B are shown for Greenland in Figure 4.6 and for Antarctica in Figure 4.7. The figures also provide information on the percentage of data that falls into each surface class.

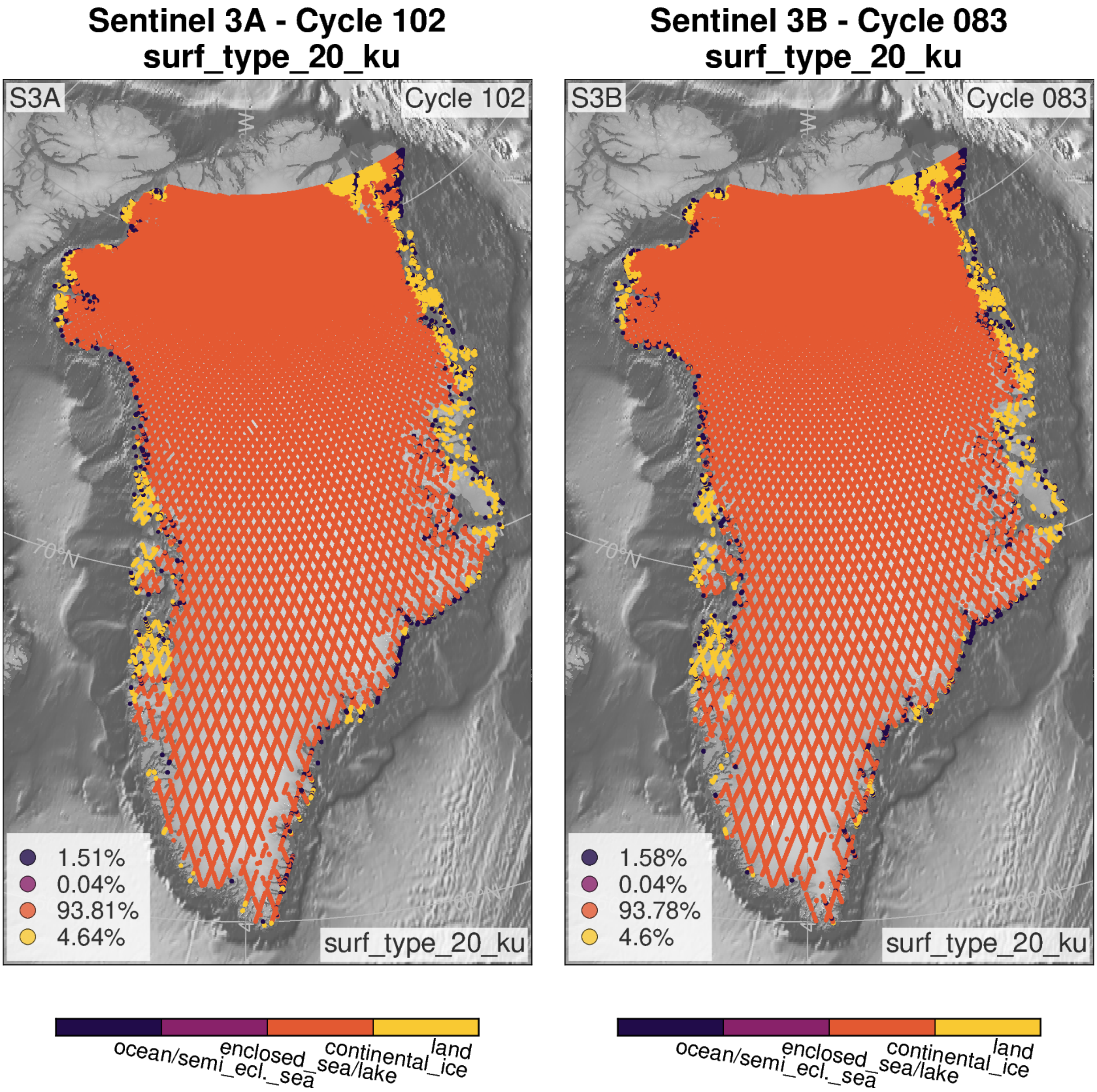

Figure 4.4 Surface Type for Greenland ice sheet from the surf_type_20_ku parameter

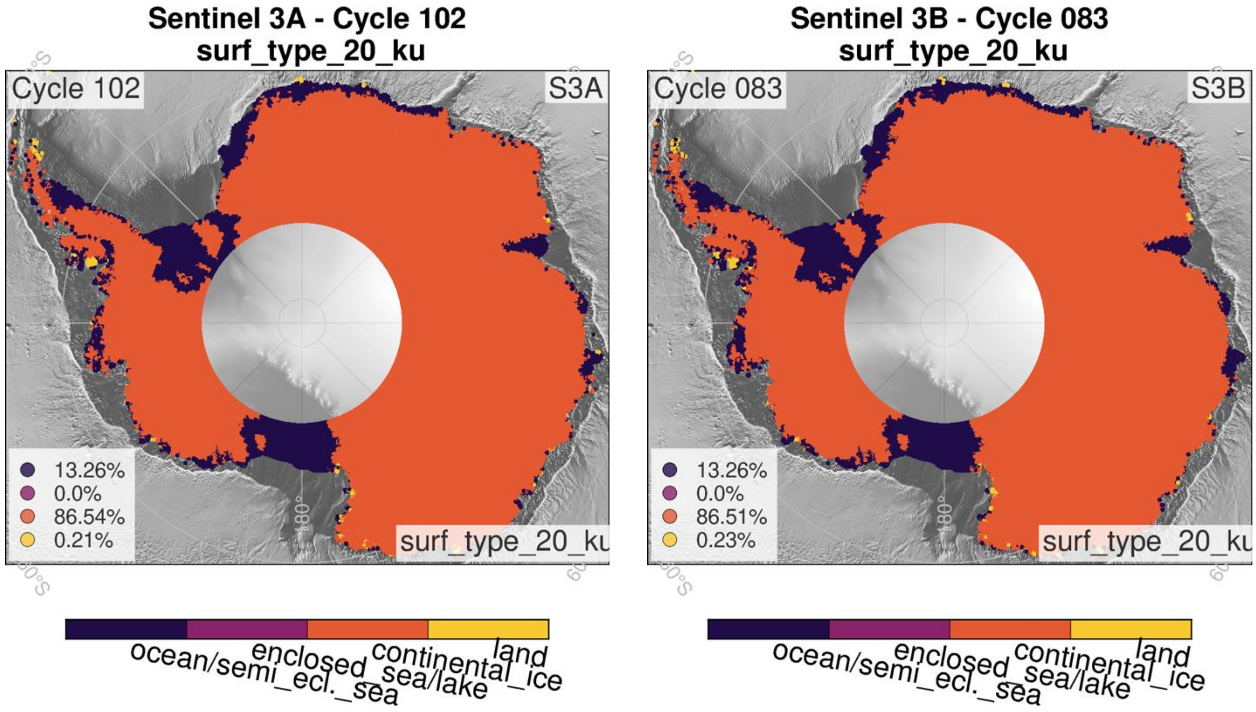

Figure 4.5 Surface Type for Antarctic Ice Sheet and Ice cap from the surf_type_20_ku parameter

4.4.2 20 Hz Ku Band Surface Class (surf_class_20_ku)

The 20 Hz Ku surface classification parameter (surf_class_20_ku) is derived from MODIS and GlobCover data. The possible surface classes are: Open ocean, Land, Continental water, Aquatic vegetation, Continental ice, Floating ice, and Salt basins. The surf_class_20_ku parameter for the current cycles of S3A and S3B are shown for Greenland in Figure 4.6 and for Antarctica in Figure 4.7. The figures also provide information on the percentage of data that falls into each surface class.

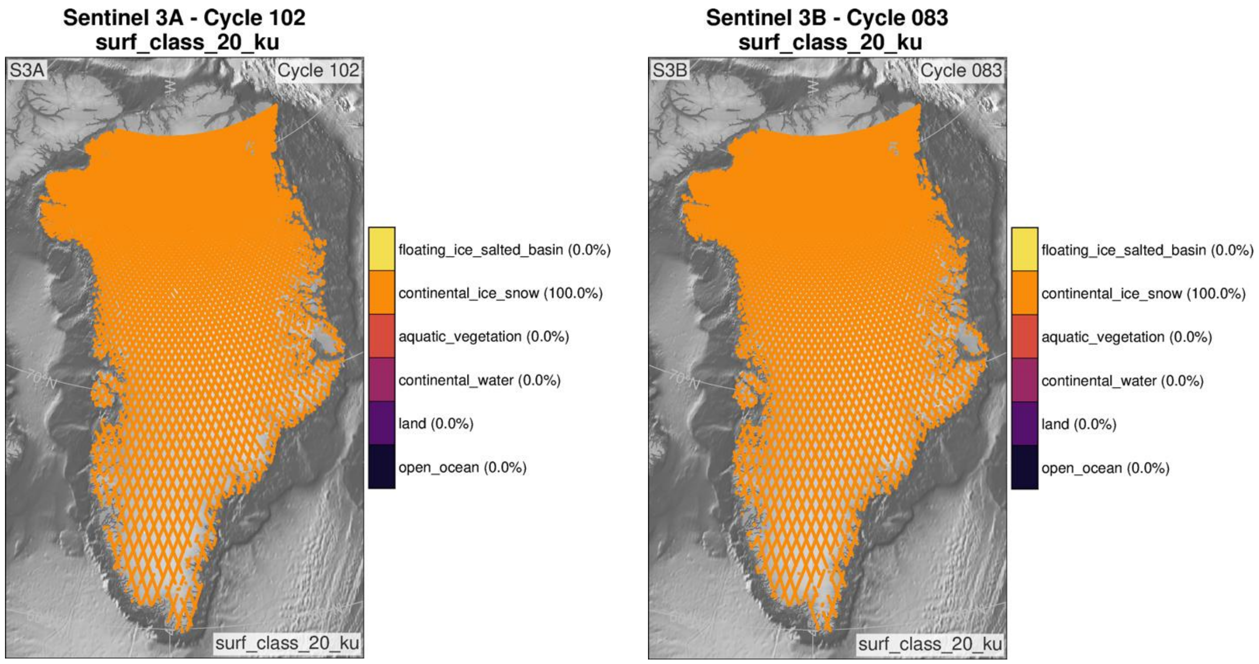

Figure 4.6 Surface Class for the Greenland ice sheet from the surf_class_20_ku parameter

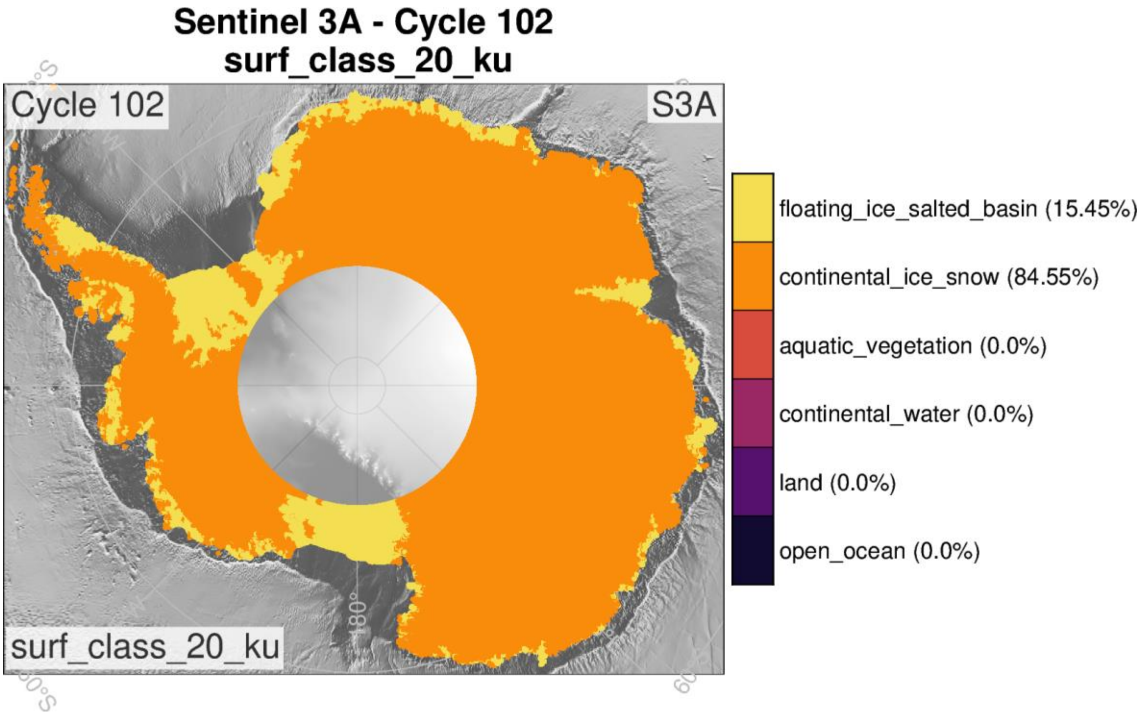

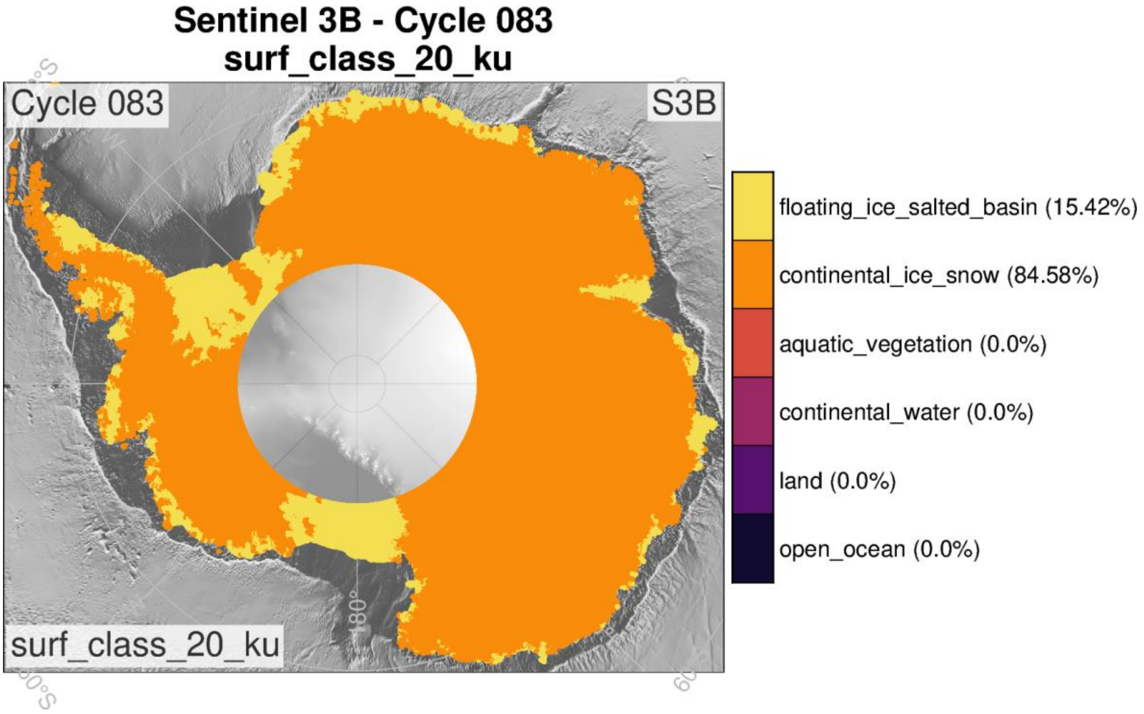

Figure 4.7 Surface Class for Antarctica from the surf_class_20_ku parameter

5 Geophysical parameters monitoring

5.1 Geophysical parameters derived from altimetry

Over land ice two different retrackers are implemented in the Sentinel-3 Instrument Processing Facilities (IPF) to retrieve geophysical parameters from SAR mode waveforms:

- The "OCOG/ICE-1 retracker" (Wingham D J, Rapley C G, and Griffiths H 1986; Bamber 1994) is an empirical algorithm commonly used over land surfaces. The OCOG/ICE-1 retracker is robust and will almost always return a topography estimation, even over rugged or steep topography, where the altimetry waveform may exhibit complex waveform shapes.
- The "UCL ice sheet retracker" is a model fit retracker, optimised for use over areas of low slope where the returned waveform has a classical shape typical of flat and smooth ice sheet surfaces. The echo model used has a modified gaussian form, corresponding to a six parameterizable function with 5-section modelling. It has a heritage from the CryoSat-2 mission's Wingham/Wallis retracker (Wingham and Wallis 2010).

Two main geophysical parameters are derived from both retrackers:

- The surface elevation with respect to the reference ellipsoid (WGS-84). Parameter's name in the level-2 LAND products are "elevation_ocog_20_ku" and "elevation_ice_sheet_20_ku", respectively estimated with the "OCOG/ICE-1" and "UCL ice sheet" retrackers.
- The backscattering coefficient (Sigma-0). Parameter's name in the level-2 LAND products are "sig0_ocog_20_ku" and "sig0_ice_sheet_20_ku", respectively estimated with the "OCOG/ICE-1" and "UCL ice sheet" retrackers. The backscatter values are controlled by surface characteristics, such as slope, roughness, and surface properties (volume vs. surface scattering). It is an important parameter and is used for deriving accurate estimates of ice/snow surface elevation changes.

In addition, the altimeter range and backscattering coefficient derived from the Pseudo-LRM (PLRM) waveforms are also available in the level-2 products assessed. They are retrieved by the ICE-2 retracker (Legresy and Remy 1997). Parameter's names are respectively "range_ice_20_plrm_ku" and "sig0_ice_20_plrm_ku".

5.1.1 20 Hz Ku Band Elevation (elevation_ice_sheet_20_ku)

Figure 5.1 shows the elevation_ice_sheet_20_ku parameter over the Greenland ice sheet for the S3A and S3B full cycles, while Figure 5.2 shows the percentage of parameter failure (NaN reported) evaluated in 5x5 km grid cells.

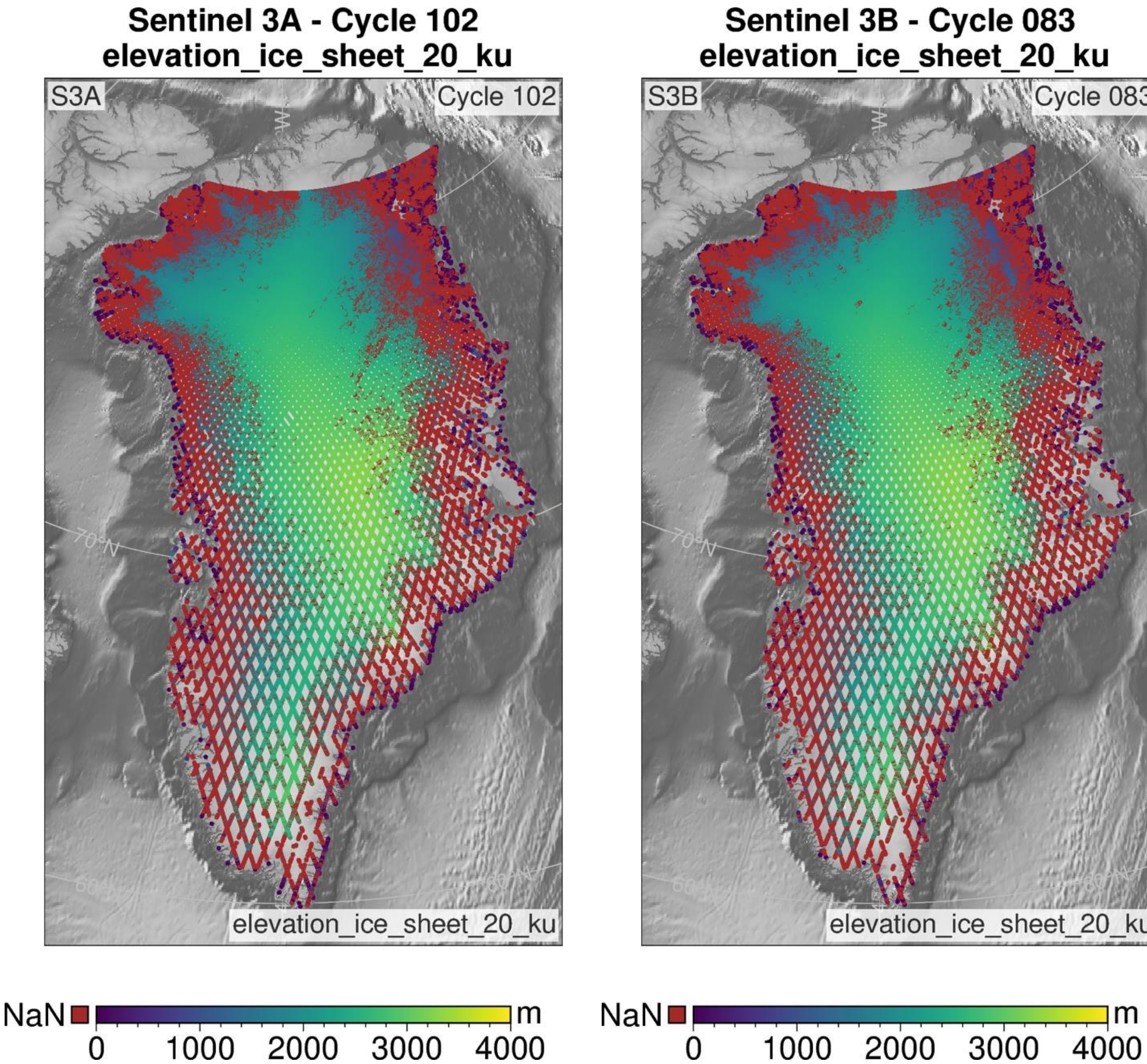

Figure 5.1 SAR mode Ice sheet elevation over Greenland from the elevation_ice_sheet_20_ku parameter

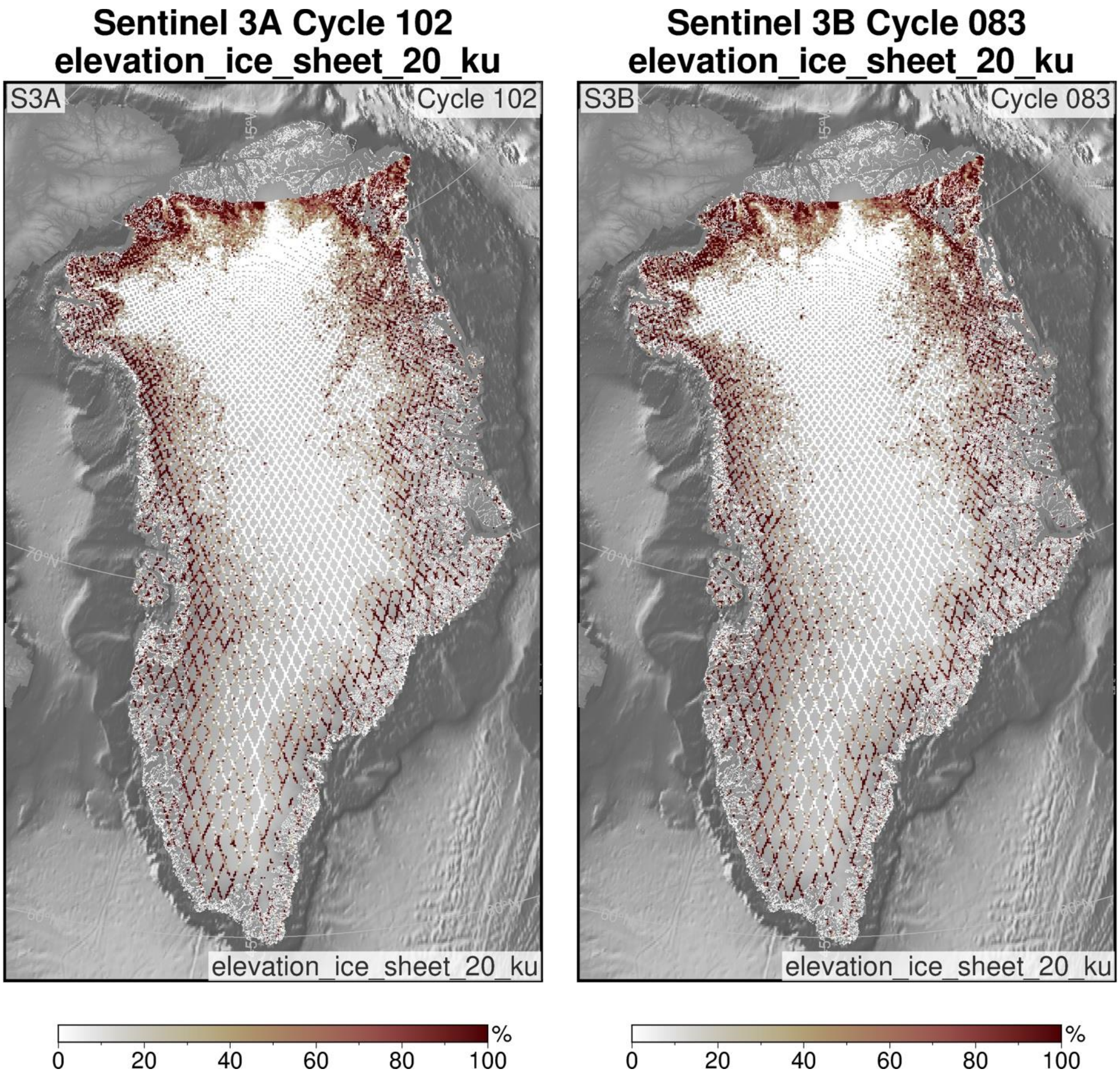

Figure 5.2 Percentage of failure over Greenland from the elevation_ice_sheet_20_ku parameter

Figure 5.3 shows the elevation_ice_sheet_20_ku parameter over Antarctica for the S3A and S3B full cycles, while Figure 5.4 shows the percentage of parameter failure (NaN reported) evaluated in 10x10 km grid cells.

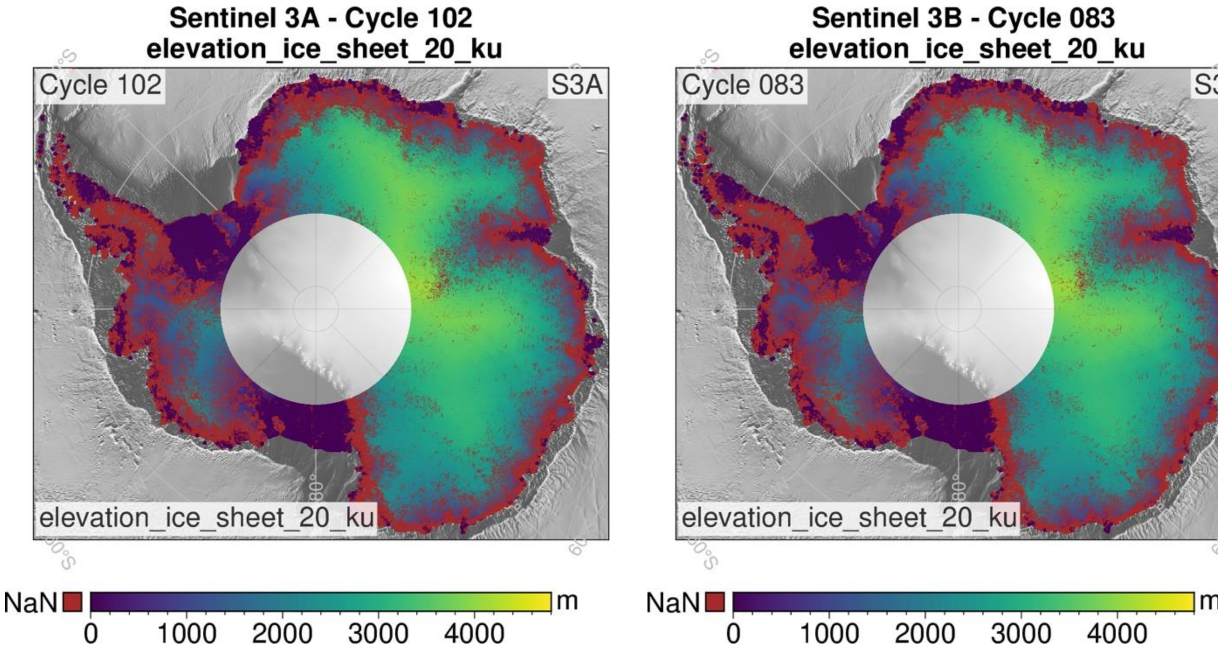

Figure 5.3 SAR mode elevation over Antarctica from the elevation_ice_sheet_20_ku parameter

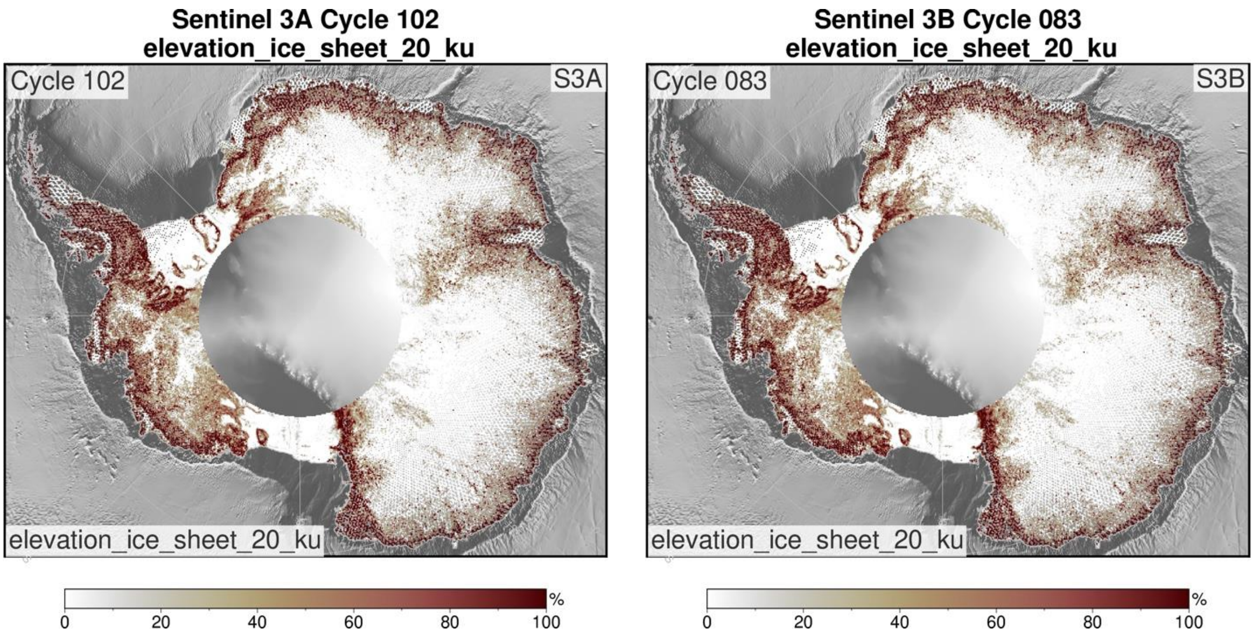

Figure 5.4 Percentage of failure over Antarctica from the elevation_ice_sheet_20_ku parameter

5.1.2 20 Hz Ku Band Ice Sheet Range (range_ice_sheet_20_ku)

Figure 5.5 shows the range_ice_sheet_20_ku_parameter over the Greenland ice sheet for the S3A and S3B full cycles, while Figure 5.6 shows the percentage of parameter failure (NaN reported) evaluated in 5x5 km grid cells. Figure 5.7 shows the range_ice_sheet_20_ku parameter over the Antarctic ice sheets for the S3A and S3B full cycles, while Figure 5.8 shows the percentage of parameter failure (NaN reported) evaluated in 10x10km grid cells.

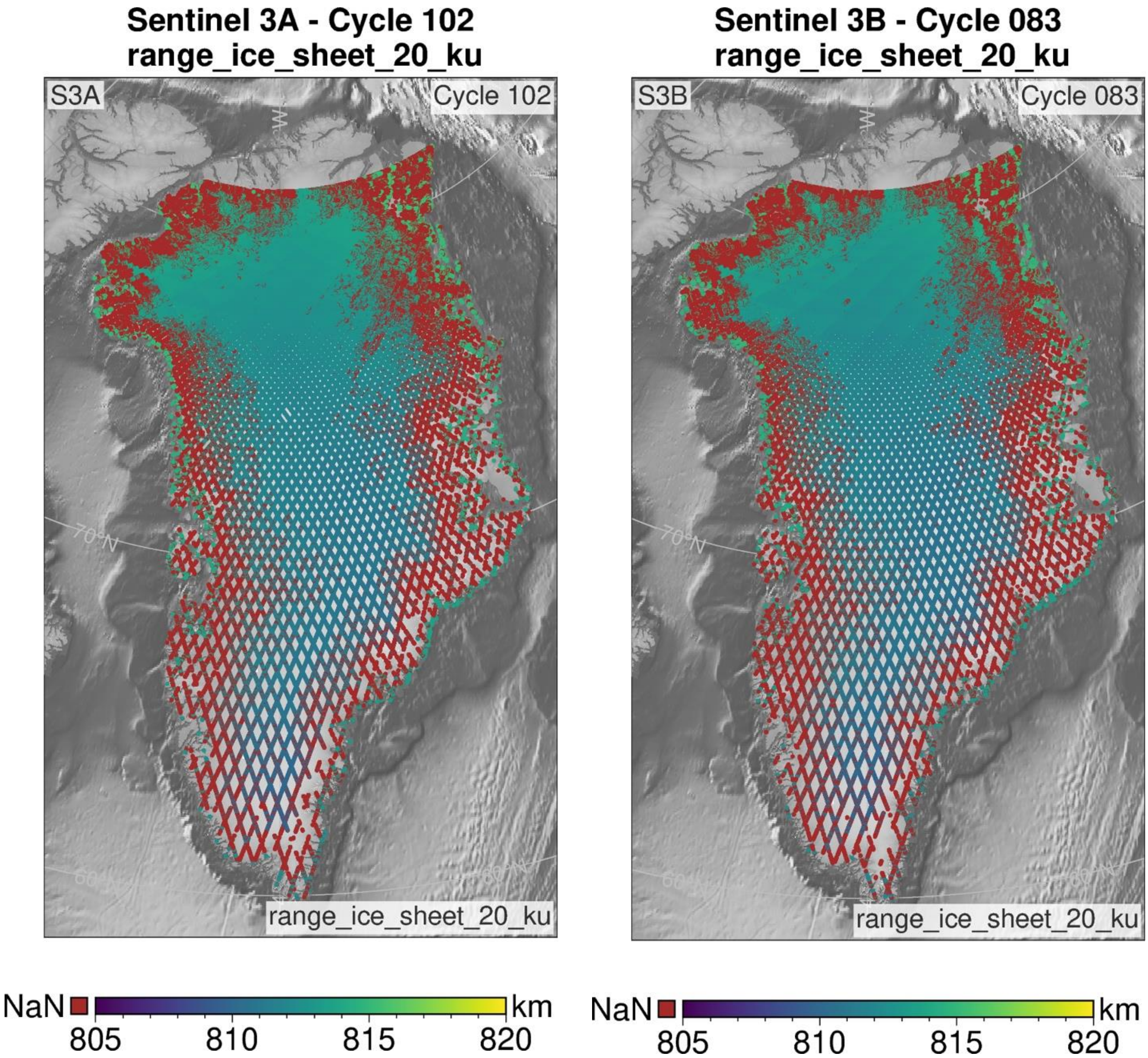

Figure 5.5 SAR mode range over the Greenland ice sheet from the range_ice_sheet_20_ku parameter

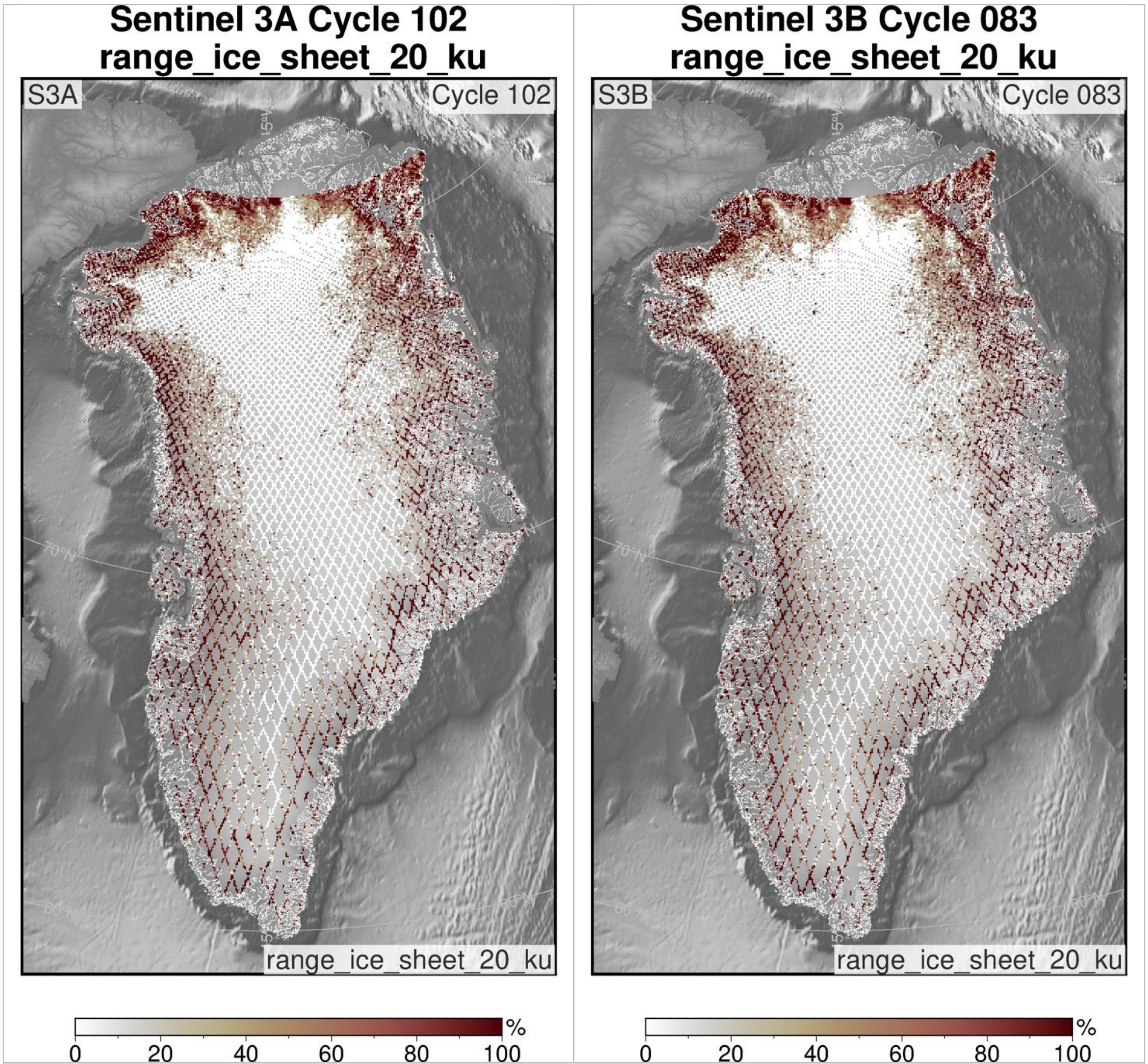

Figure 5.6 Percentage of failure over the Greenland ice sheet for the range_ice_sheet_20_ku parameter

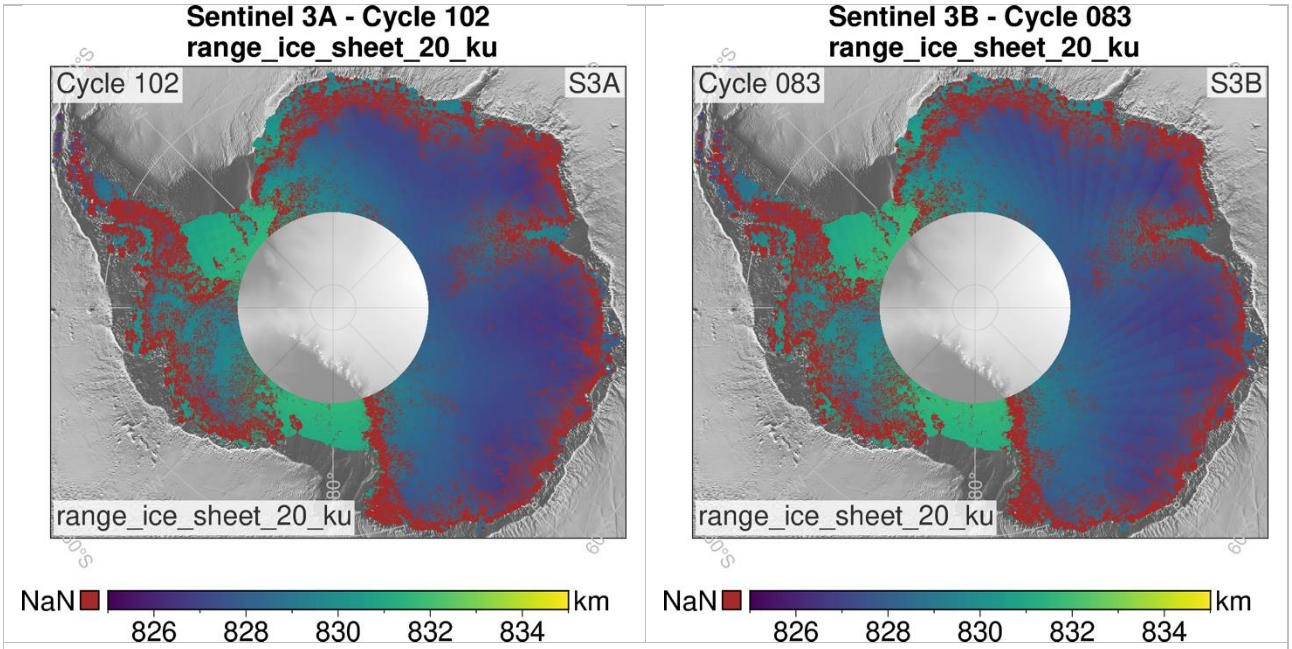

Figure 5.7 SAR mode range over Antarctica from the range_ice_sheet_20_ku parameter

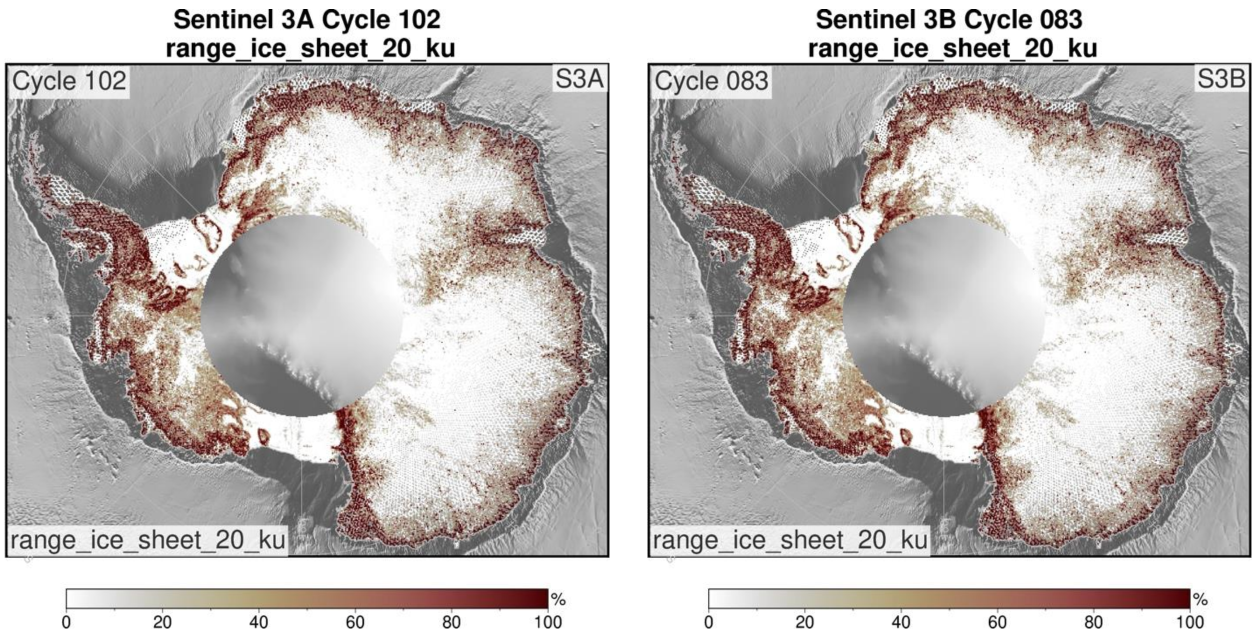

Figure 5.8 Percentage of failure over Antarctica for the range_ice_sheet parameter

5.1.3 20Hz Ku Band Ice Sheet Sigma0 (sig0_ice_sheet_20_ku)

Figure 5.9 shows the sig0_ice_sheet_20_ku parameter over the Greenland ice sheet for the S3A and S3B full cycles, while Figure 5.11 shows the percentage of parameter failure (NaN reported) evaluated in 5x5km grid cells. Figure 5.12 shows the Sigma0 ice sheet 20 Ku parameter over the Antarctic ice sheets for the S3A and S3B full cycles. Figure 5.14 shows the percentage of parameter failure (NaN reported) evaluated in 10x10 km grid cells.

The backscatter coefficient (sig0_ice_sheet_20_ku) distribution over the Greenland Ice Sheet, and statistics given by the Number of Observations, Median (dB), Median Absolute Deviation (MAD) in dB, and the Interquartile Range (IQR) given in dB. Figure 5.10 and Figure 5.13 show the distribution and statistics of the sig0_ice_sheet_20_ku parameter for the Greenland Ice Sheet and Antarctica, respectively. For the Median Absolute Deviation (MAD) a non-normal distribution is assumed.

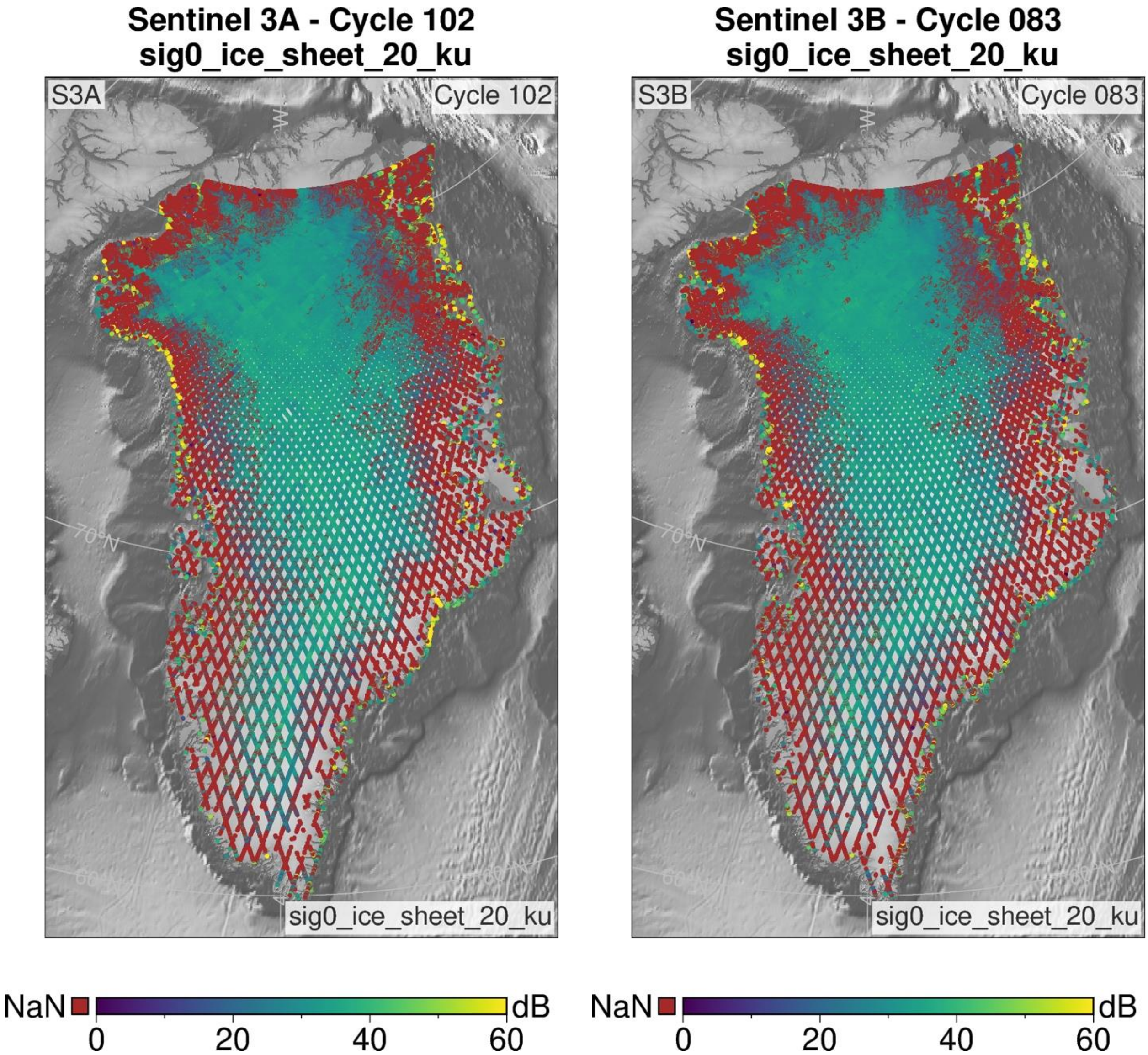

Figure 5.9 SAR mode backscatter coefficient over the Greenland ice sheet from the sig0_ice_sheet_20_ku

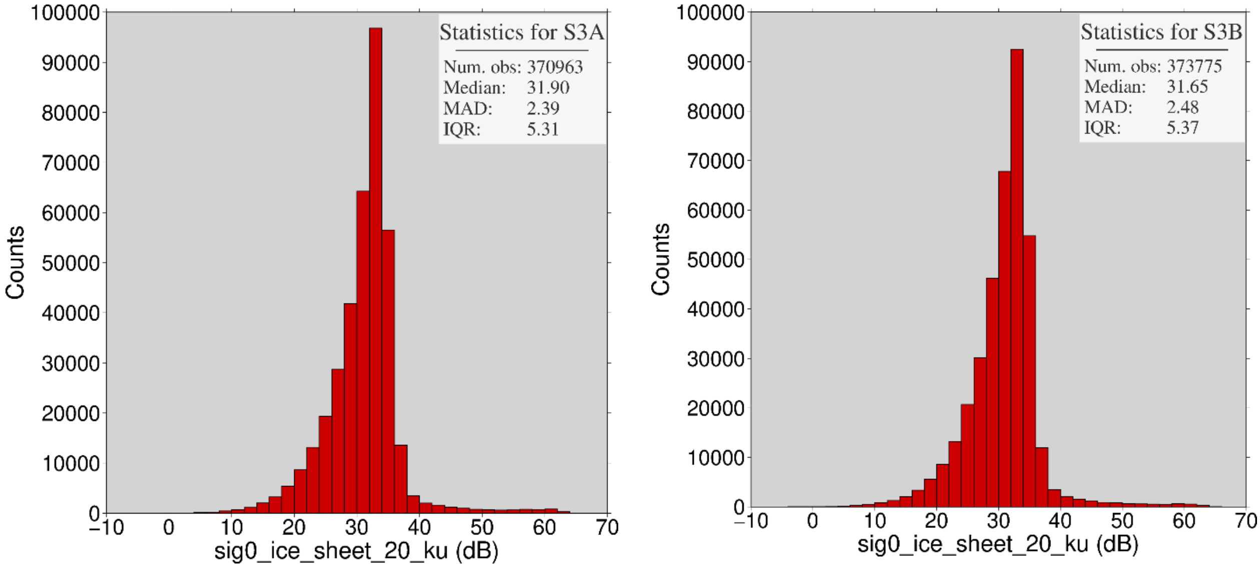

Figure 5.10 The SAR mode backscatter coefficient (sig0_ice_sheet_20_ku) distribution over the Greenland Ice Sheet, and statistics given by the Number of Observations, Median (dB), Median Absolute distribution (MAD) in dB, and the Interquartile Range (IQR) given in dB.

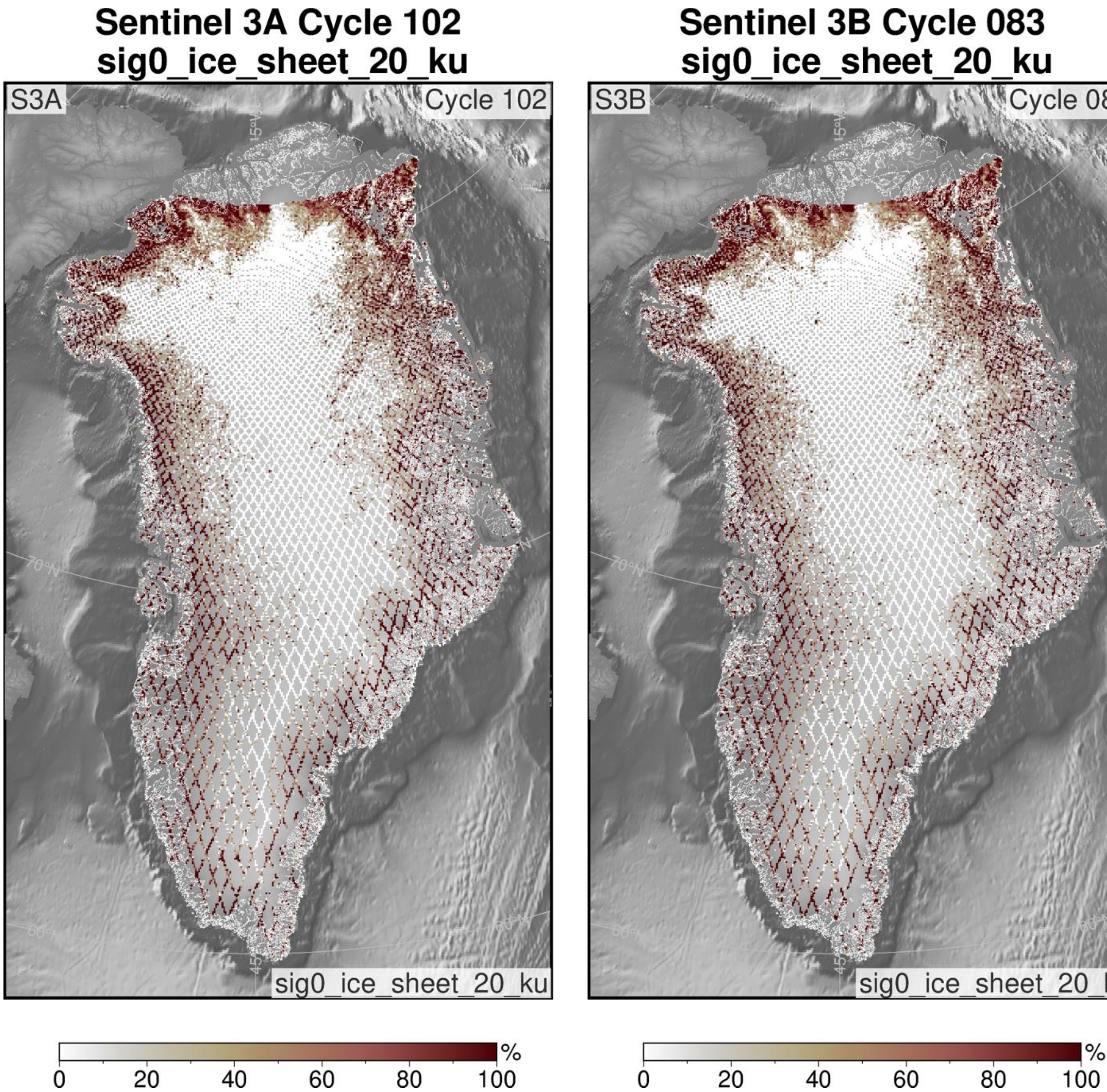

Figure 5.11 Percentage of failure over the Greenland ice sheet for the sig0_ice_sheet_20_ku parameter

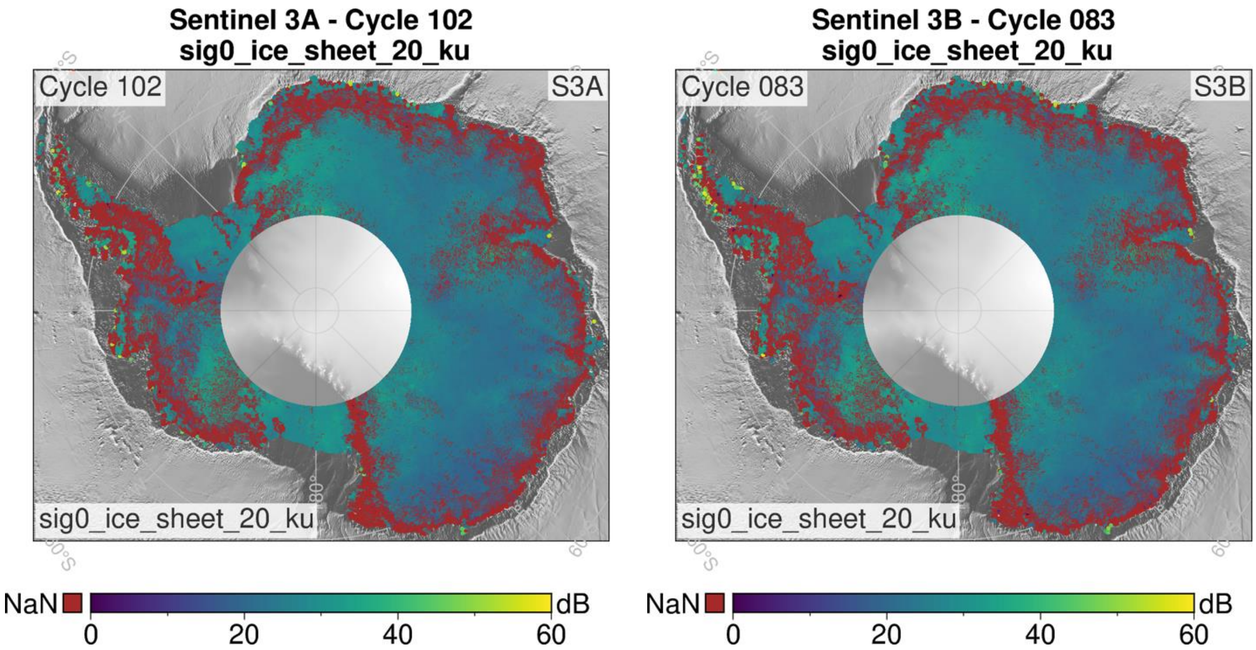

Figure 5.12 SAR mode backscatter coefficient over Antarctica from the sig0_ice_sheet_20_ku parameter

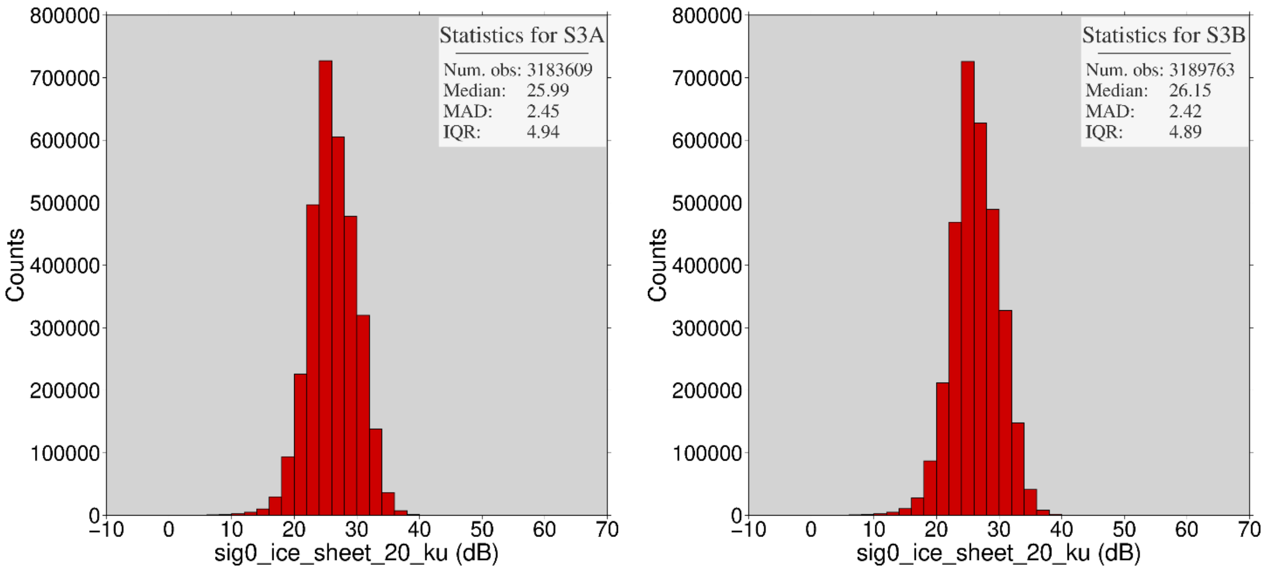

Figure 5.13 The SAR mode backscatter coefficient (sig0_ice_sheet_20_ku) distribution over Antarctica and statistics given by the Number of Observations, Median (dB), Median Absolute distribution (MAD) in dB, and the Interquartile Range (IQR) given in dB.

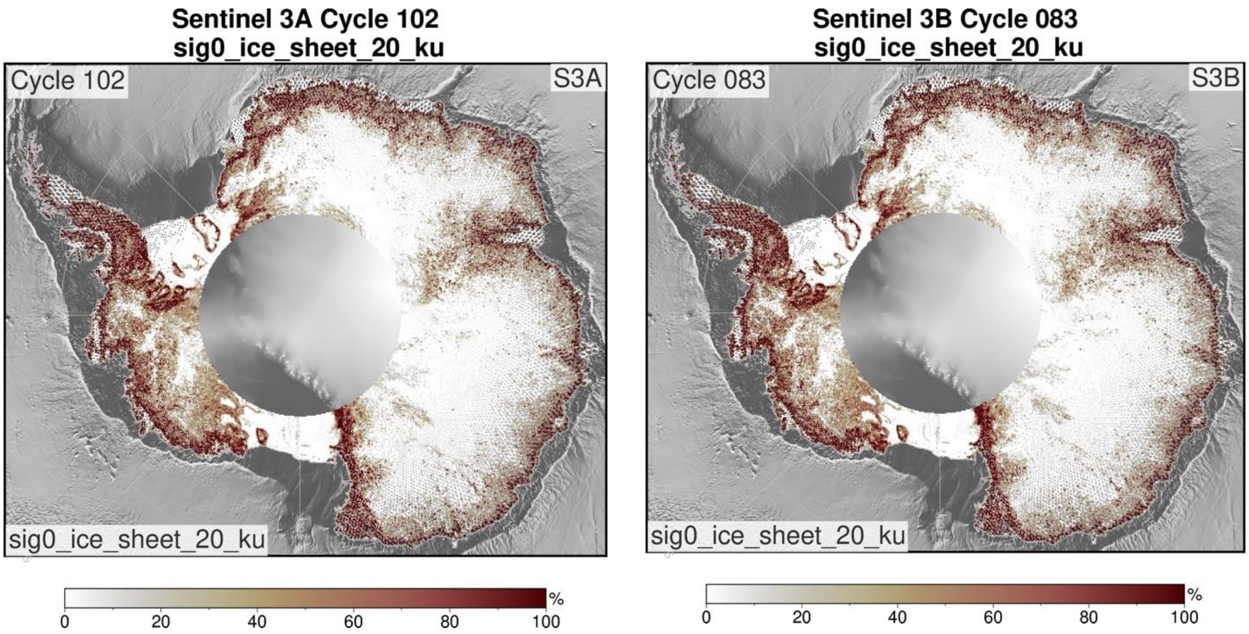

Figure 5.14 Percentage of failure over Antarctica for the sig0_ice_sheet_20_ku parameter

5.1.4 20 Hz Ku Band OCOG (Ice-1) Elevation (elevation_ocog_20_ku)

Figure 5.15 shows the elevation_ocog_20_ku parameter over the Greenland ice sheet for the S3A and S3B full cycles, while Figure 5.16 shows the percentage of parameter failure (NaN reported) evaluated in 5x5 km grid cells. Figure 5.17 shows the elevation_ice_sheet_20_ku parameter over the Antarctic ice sheets for the S3A and S3B full cycles, while Figure 5.18 shows the percentage of parameter failure (NaN reported) evaluated in 10x10 km grid cells.

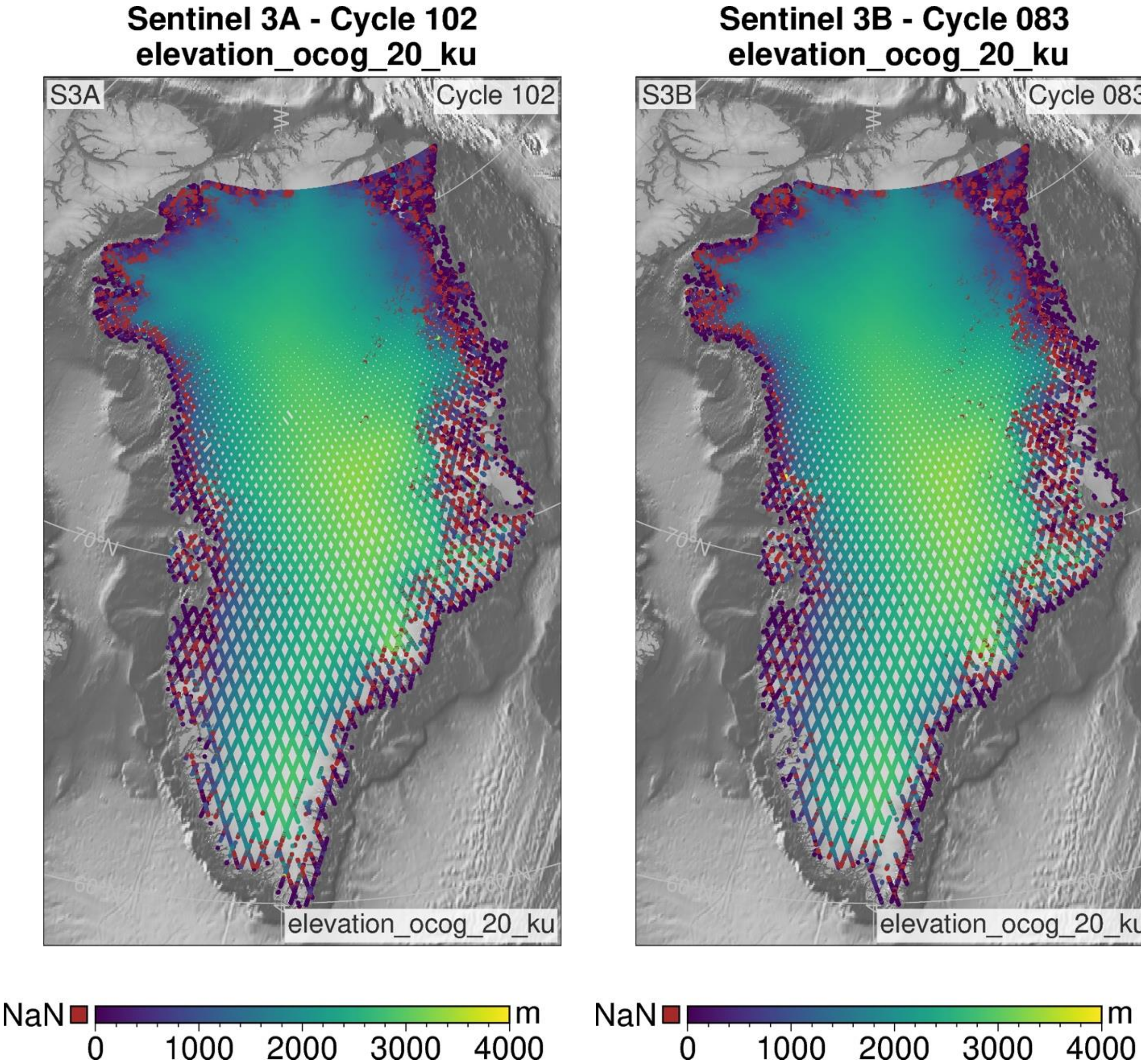

Figure 5.15 SAR mode elevation over the Greenland ice sheet from the elevation_ocog_20_ku parameter

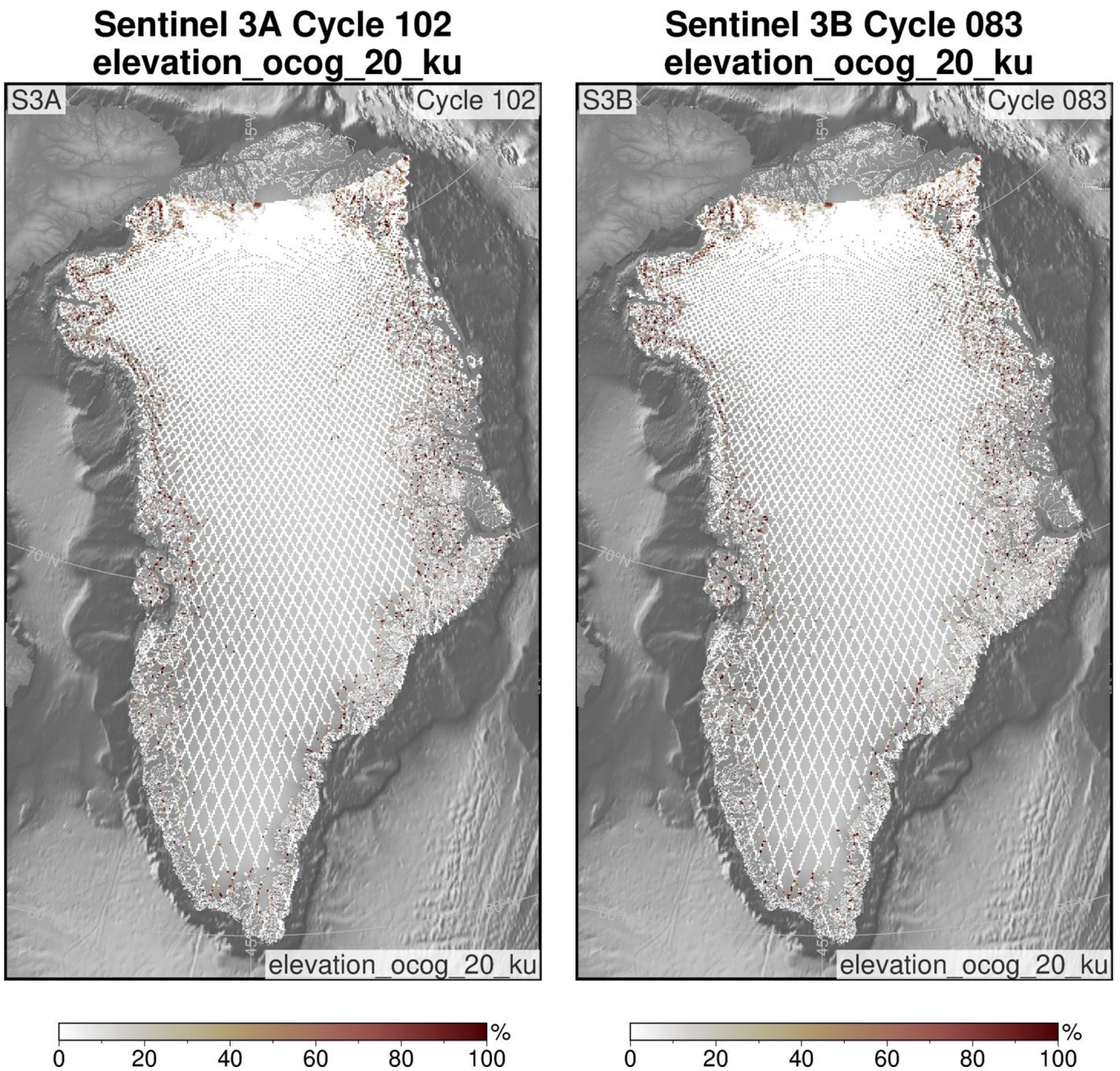

Figure 5.16 Percentage of failure over the Greenland ice sheet for the elevation_ocog_20_ku parameter

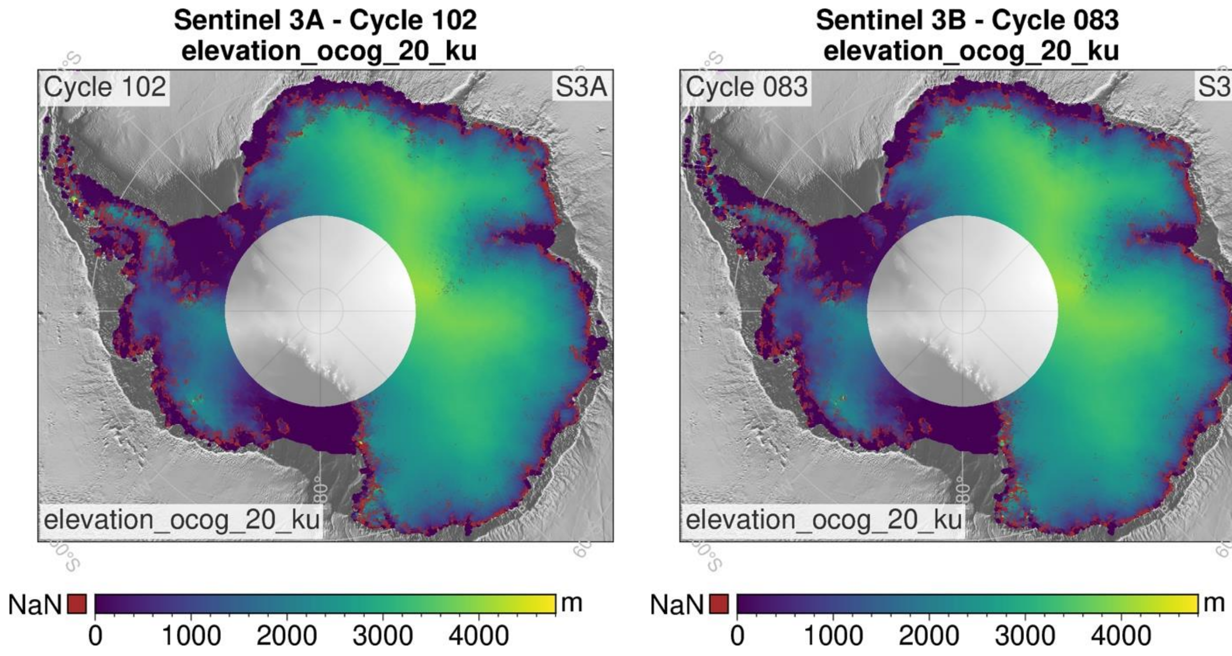

Figure 5.17 SAR mode elevation over Antarctica from the elevation_ocog_20_ku parameter

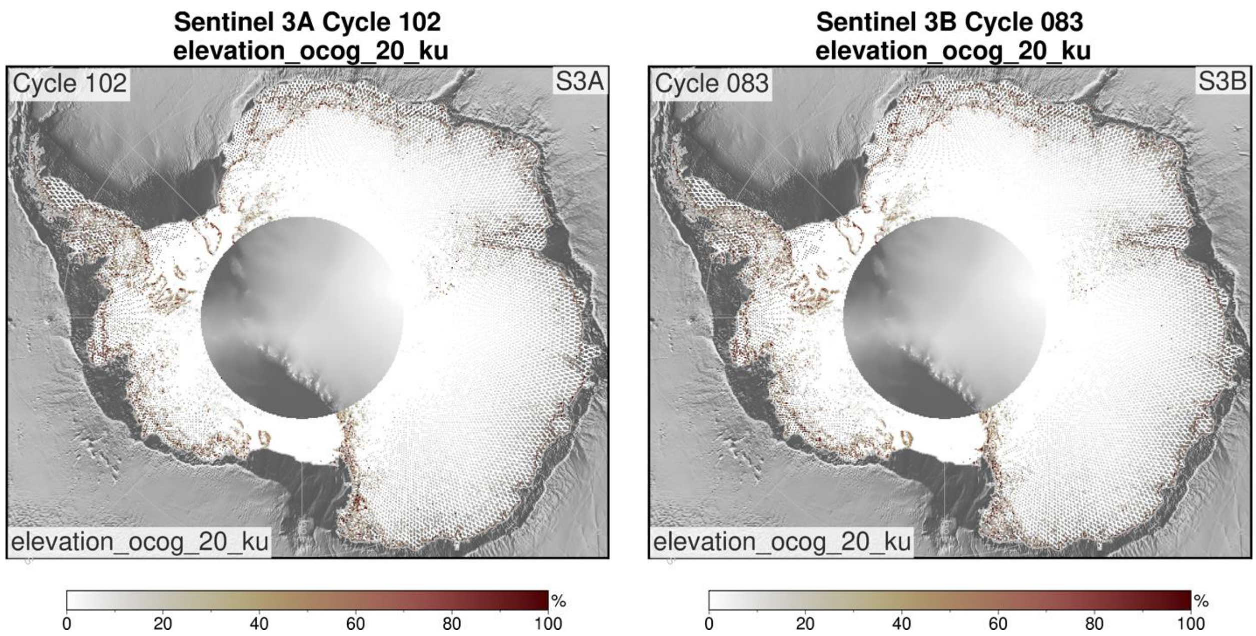

Figure 5.18 Percentage of failure over Antarctica for the elevation_ocog_20_ku parameter

5.1.5 8 20 Hz Ku Band OCOG (Ice-1) Sigma0 (sig0_ocog_20_ku)

Figure 5.19 shows the sig0_ocog_20_ku parameter over the Greenland ice sheet for the S3A and S3B full cycles, while Figure 5.21 shows the percentage of parameter failure (NaN reported) evaluated in 5x5 km grid cells. Figure 5.22 shows the sig0_ocog_20_ku parameter over the Antarctic ice sheets for the S3A and S3B full cycles, while Figure 5.24 shows the percentage of parameter failure (NaN reported) evaluated in 10x10 km grid cells. Figure 5.20 and Figure 5.23 show the distribution and statistics of the sig0_ice_sheet_20_ku parameter for the Greenland Ice Sheet and Antarctica, respectively. For the Median Absolute Deviation (MAD) a non-normal distribution is assumed.

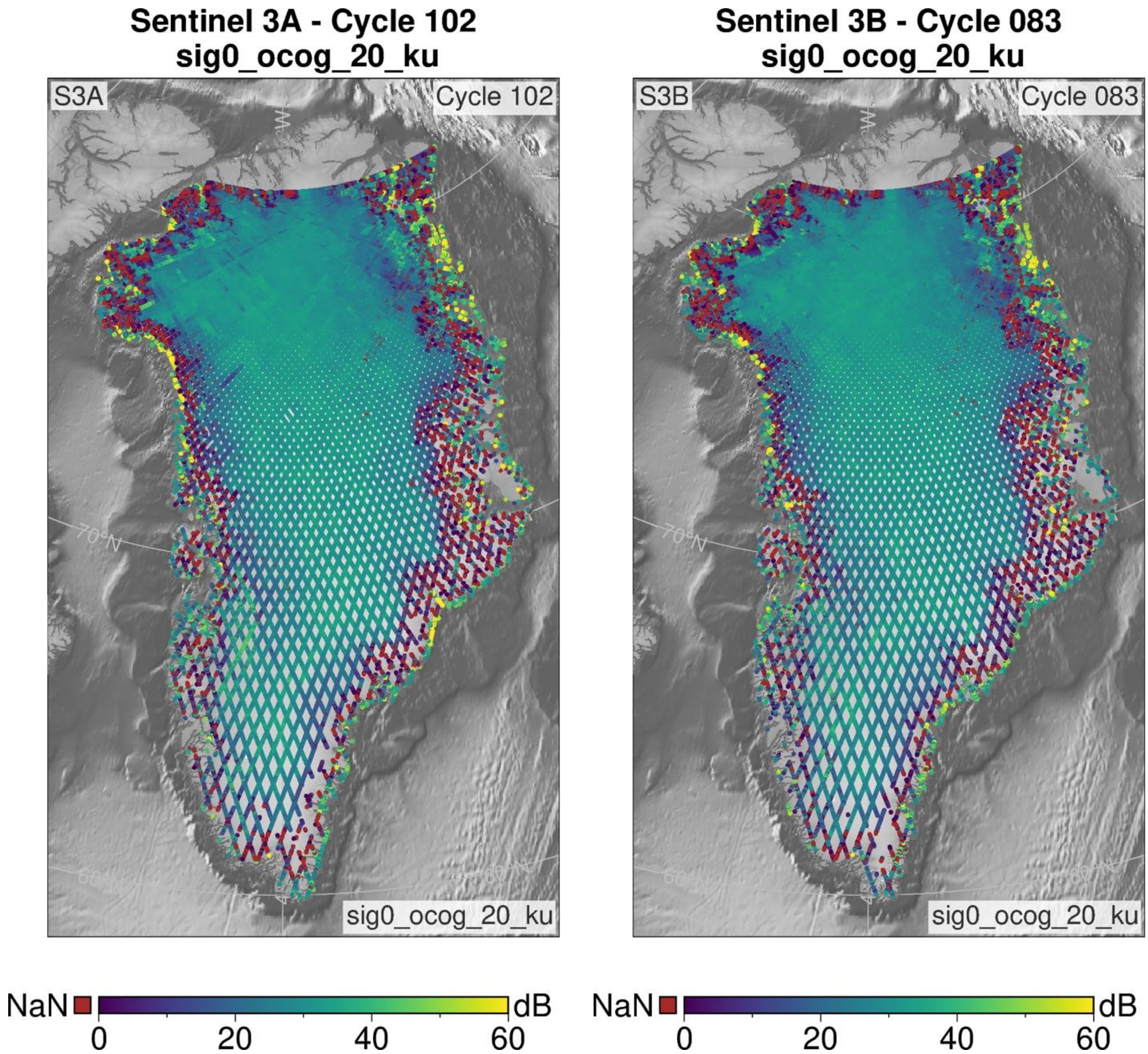

Figure 5.19 SAR mode backscatter coefficient over the Greenland ice sheet from the sig0_ocog_20_ku parameter

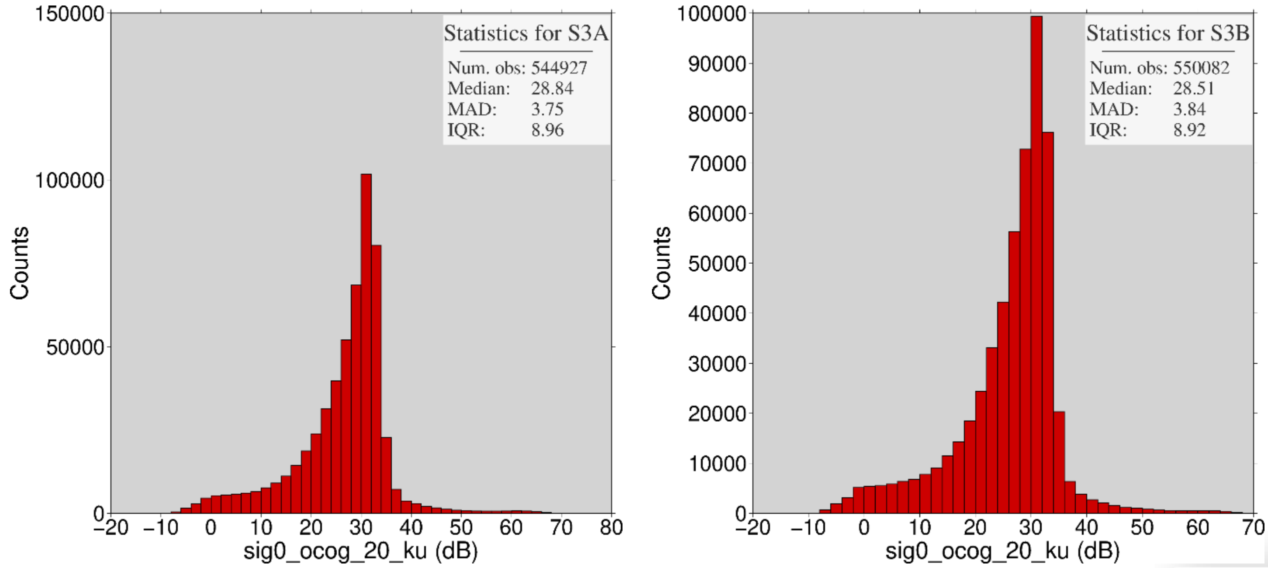

Figure 5.20 SAR mode backscatter coefficient (sig0_ice_ocog_20_ku) distribution over the Greenland Ice Sheet and statistics given by the Number of Observations, Median (dB), Median Absolute distribution (MAD) in dB, and the Interquartile Range (IQR) given in dB.

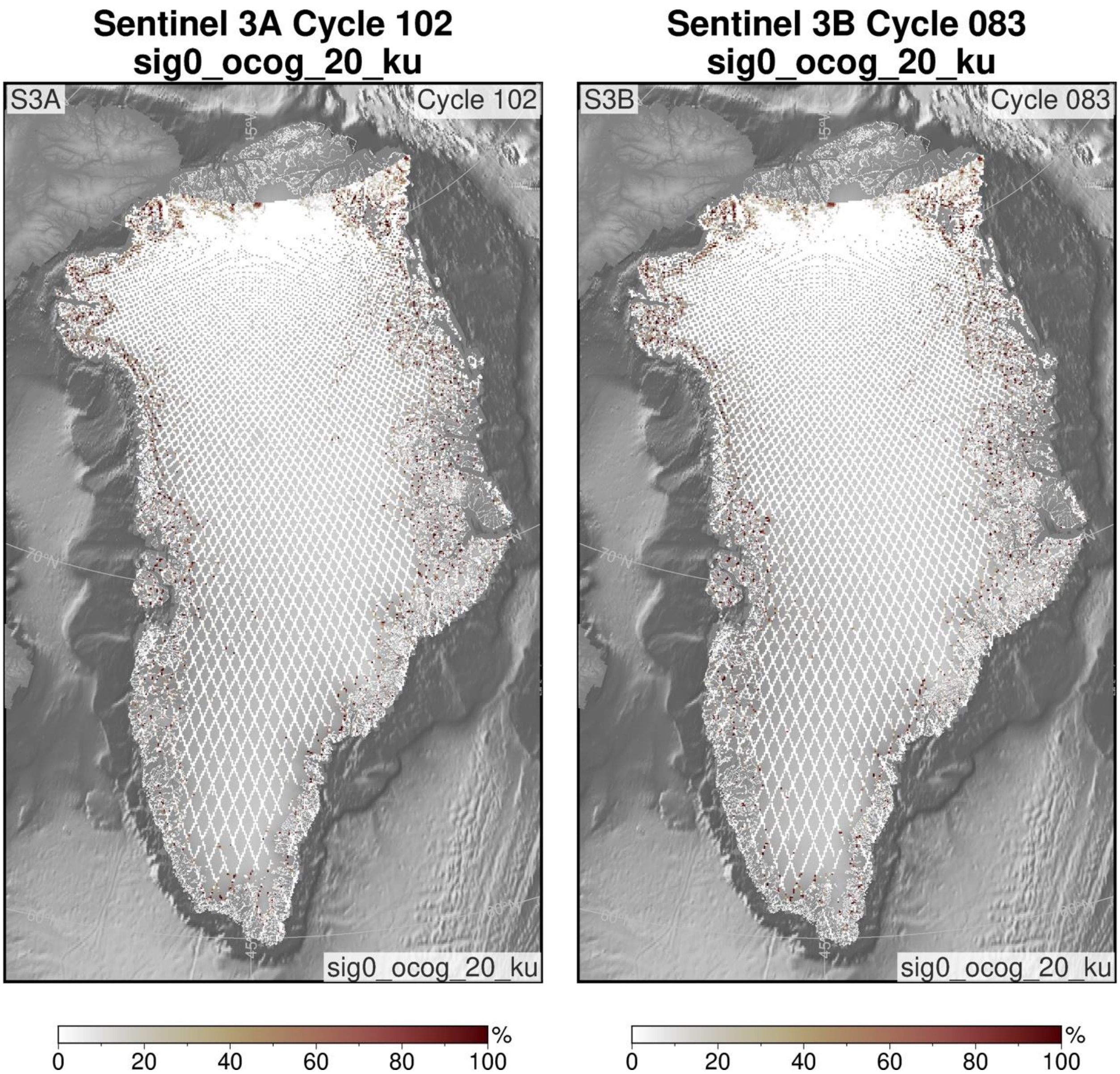

Figure 5.21 Percentage of failure over the Greenland ice sheet from the sig0_ocog_20_ku parameter

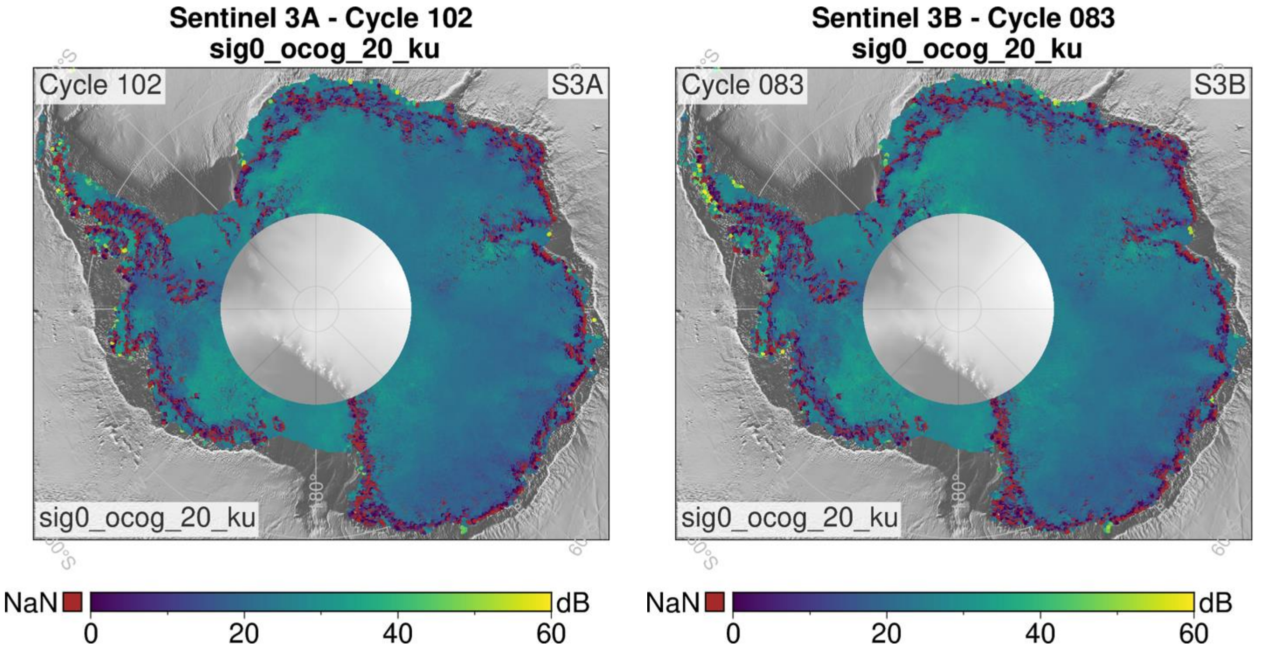

Figure 5.22 SAR mode backscatter coefficient over Antarctica from the sig0_ocog_20_ku parameter

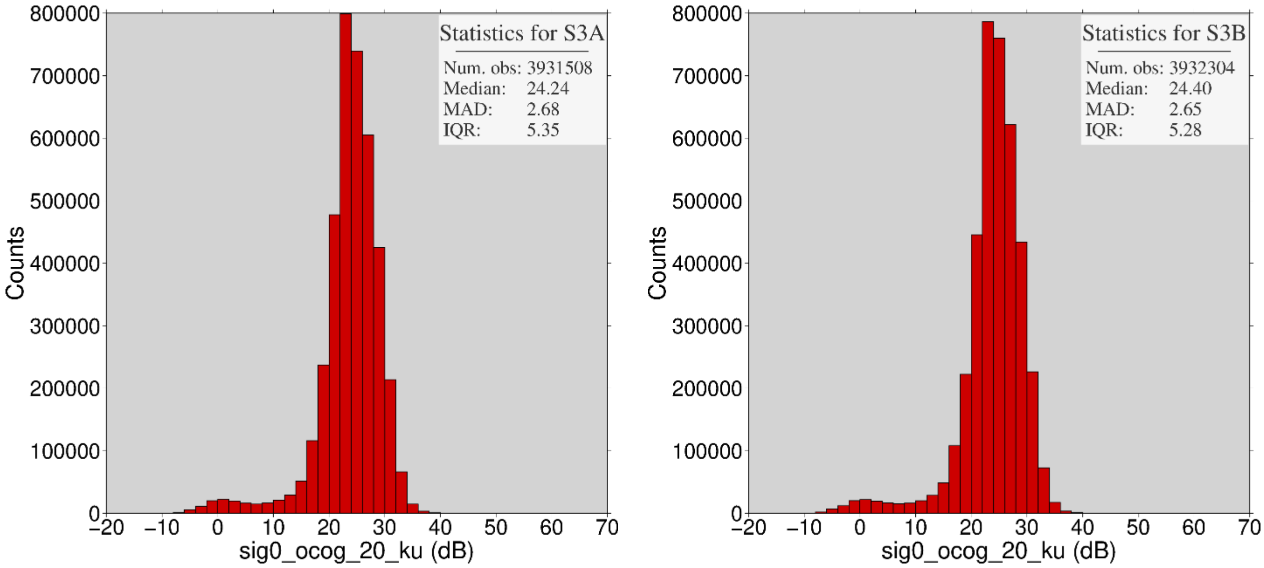

Figure 5.23 The backscatter coefficient (sig0_ocog_20_ku) distribution over Antarctica and statistics given by the Number of Observations, Median (dB), Median Absolute distribution (MAD) in dB, and the Interquartile Range (IQR) given in dB.

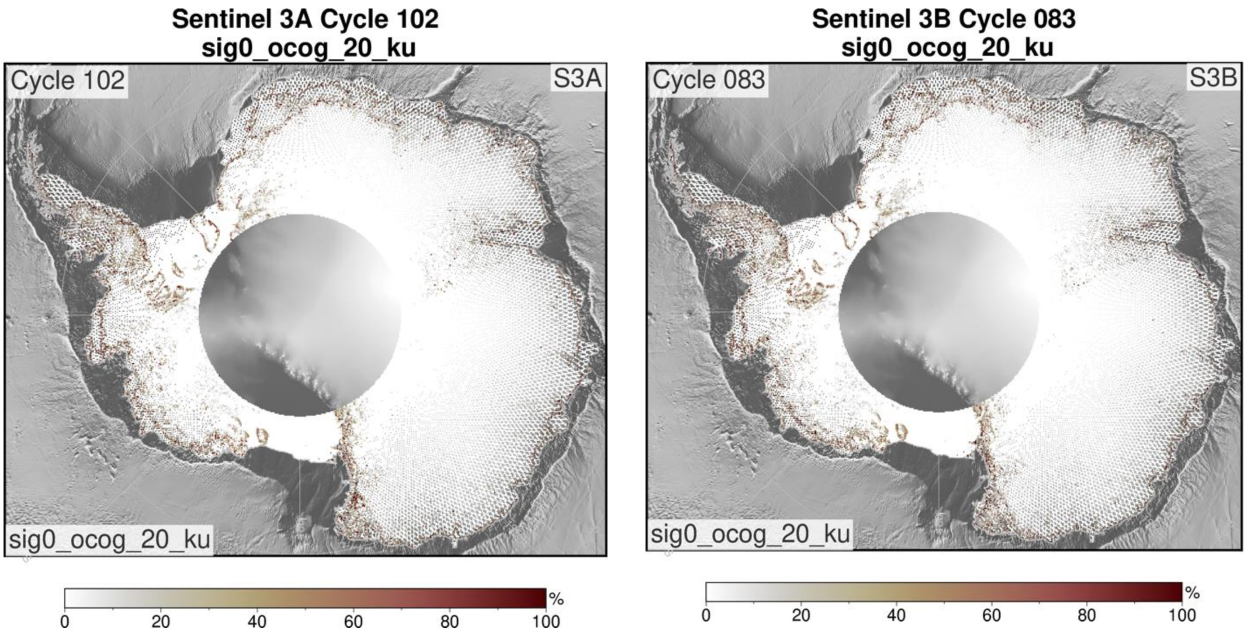

Figure 5.24 Percentage of failure over Antarctica for the sig0_ocog_20_ku parameter

5.1.6 20 Hz Ku Band OCOG (Ice-1) Range (range_ocog_20_ku)

Figure 5.25 shows the range_ocog_20_ku parameter over the Greenland ice sheet for the S3A and S3B full cycles, while Figure 5.26 shows the percentage of parameter failure (NaN reported) evaluated in 5x5 km grid cells. Figure 5.27 shows the range_ocog_20_ku parameter over the Antarctic ice sheets for the S3A and S3B full cycles, while Figure 5.28 shows the percentage of parameter failure (NaN reported) evaluated in 10x10 km grid cells.

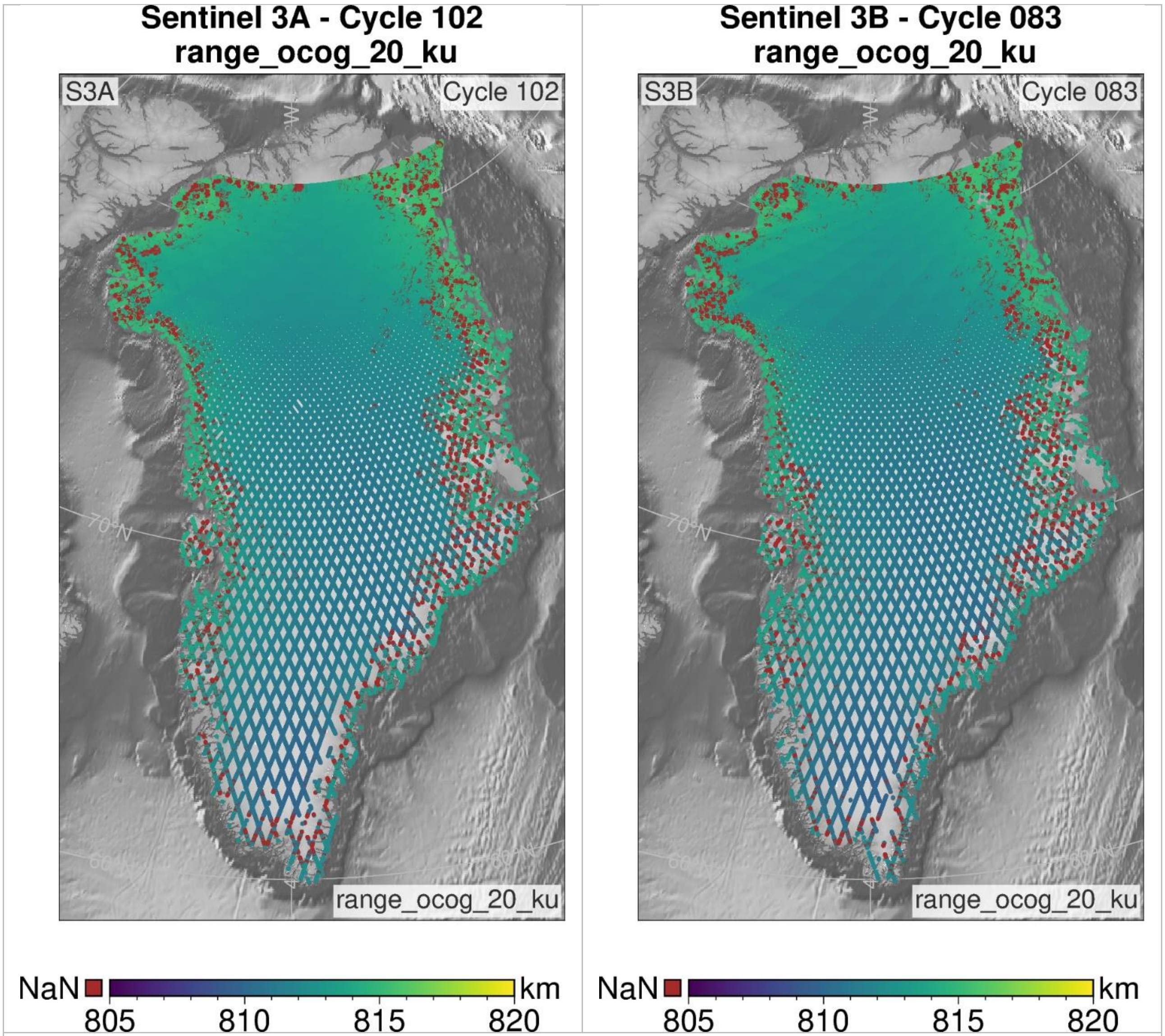

Figure 5.25 SAR mode range over the Greenland ice sheet from the range_ocog_20_ku parameter

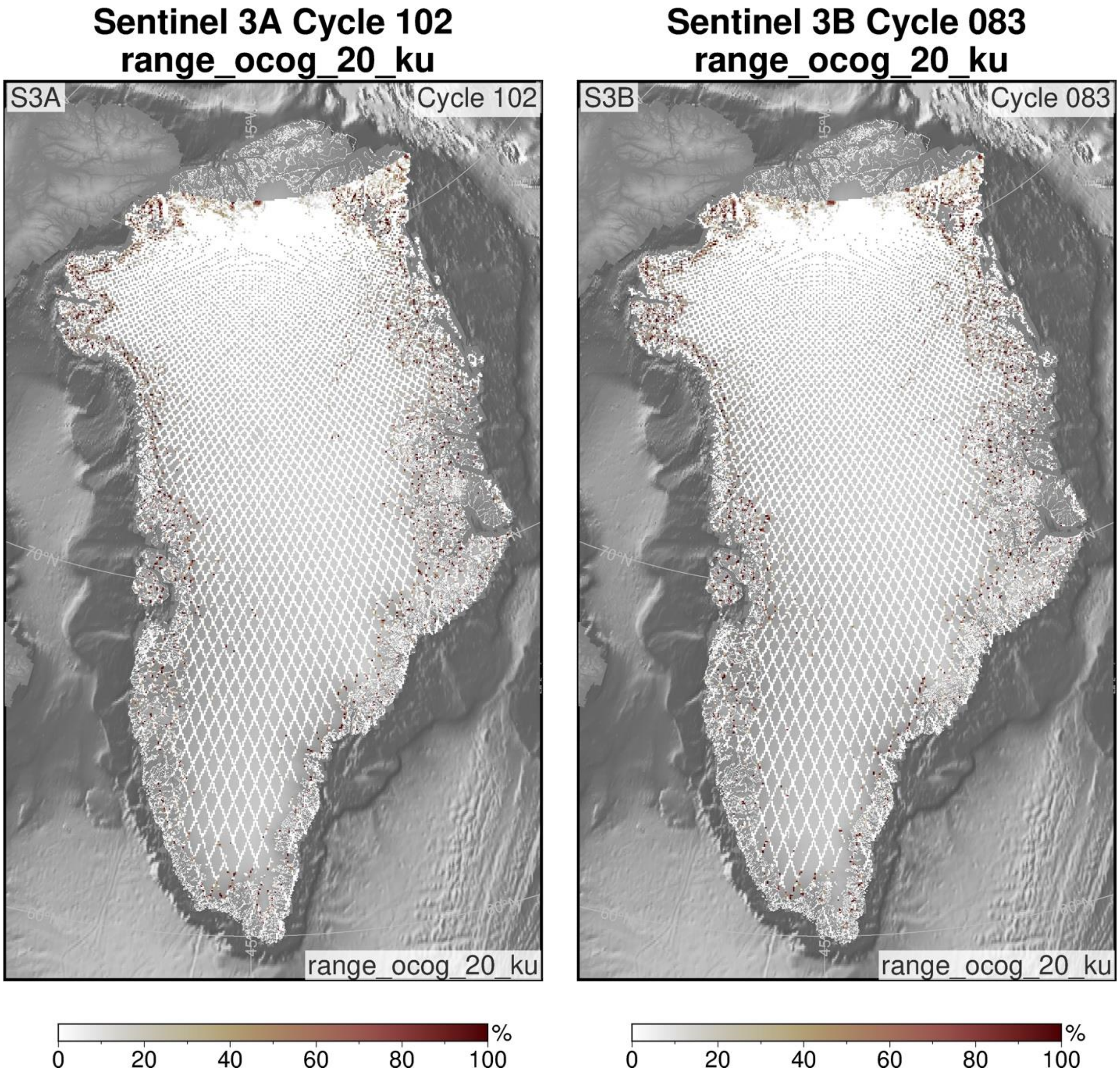

Figure 5.26 Percentage of failure over the Greenland ice sheet for the range_ocog_20_ku parameter

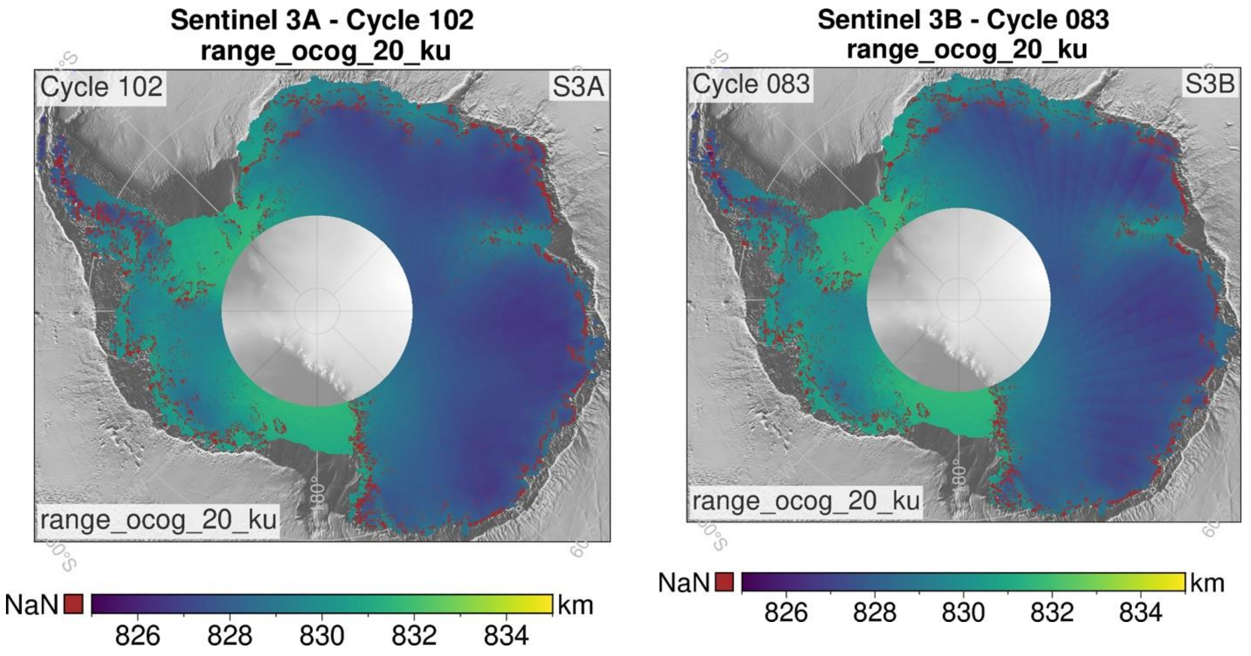

Figure 5.27 SAR Mode range over Antarctica from the range_ocog_20_ku parameter

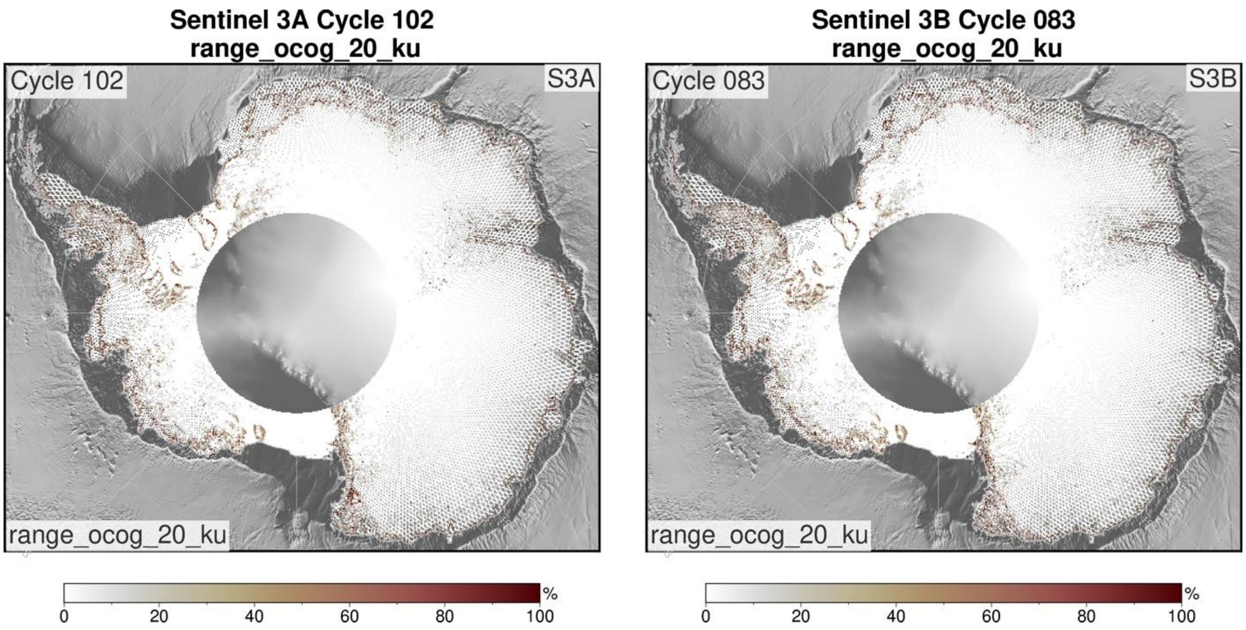

Figure 5.28 Percentage of failure over Antarctica for the range_ocog_20_ku parameter

5.1.7 PLRM Ice Range (range_ice_20_plrm_ku)

The PLRM range over the Greenland ice sheet and the Antarctic ice sheets are shown in Figure 5.29 and Figure 5.31, respectively. Their respective percentage of parameter failure (NaN reported) is shown in Figure 5.30 and Figure 5.32. The latter is evaluated in 5x5 km grid cells in Greenland and in 10x10 km grid cells in Antarctica.

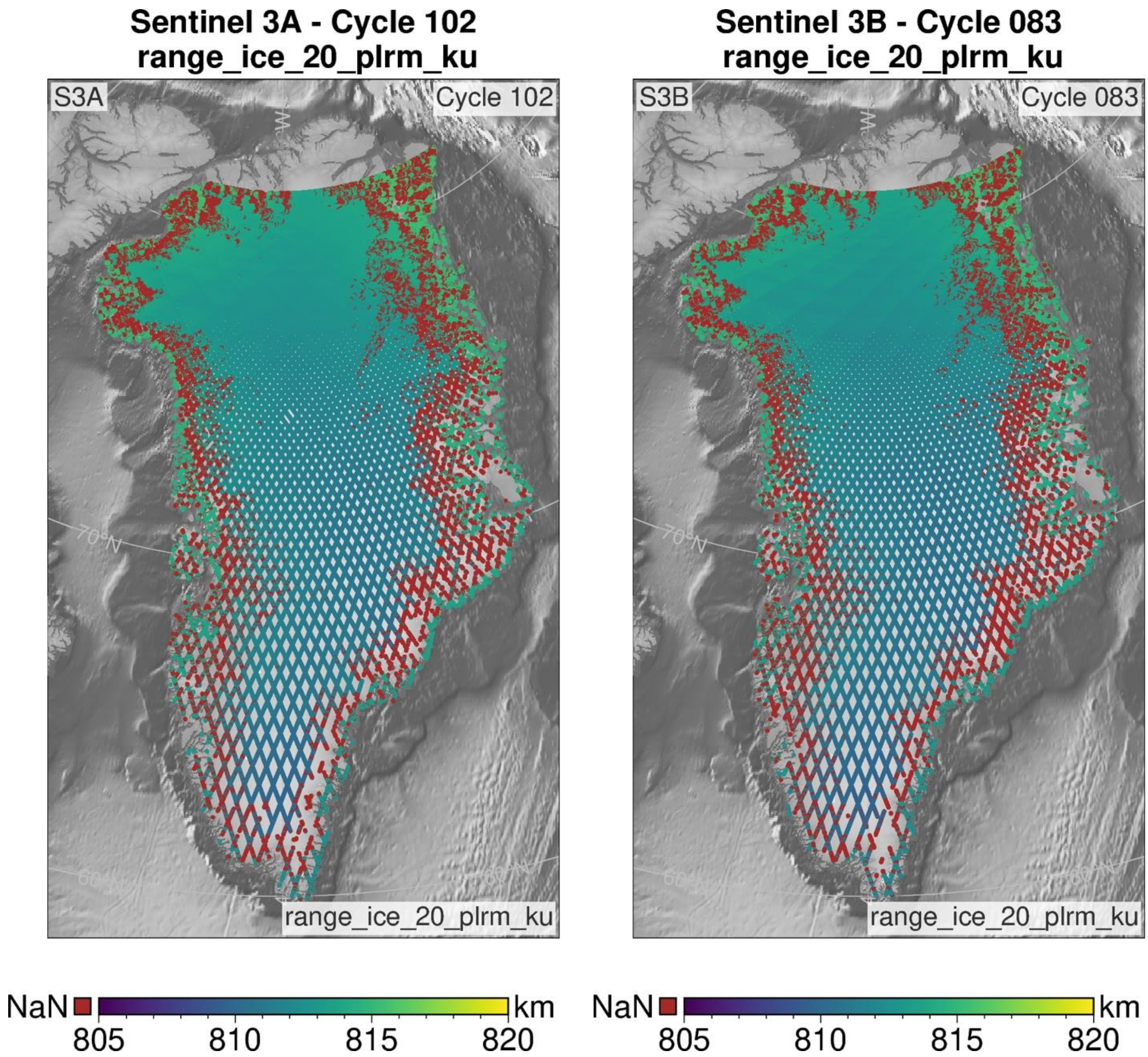

Figure 5.29 PLRM range over the Greenland Ice sheet from the range_ice_20_plrm_ku parameter

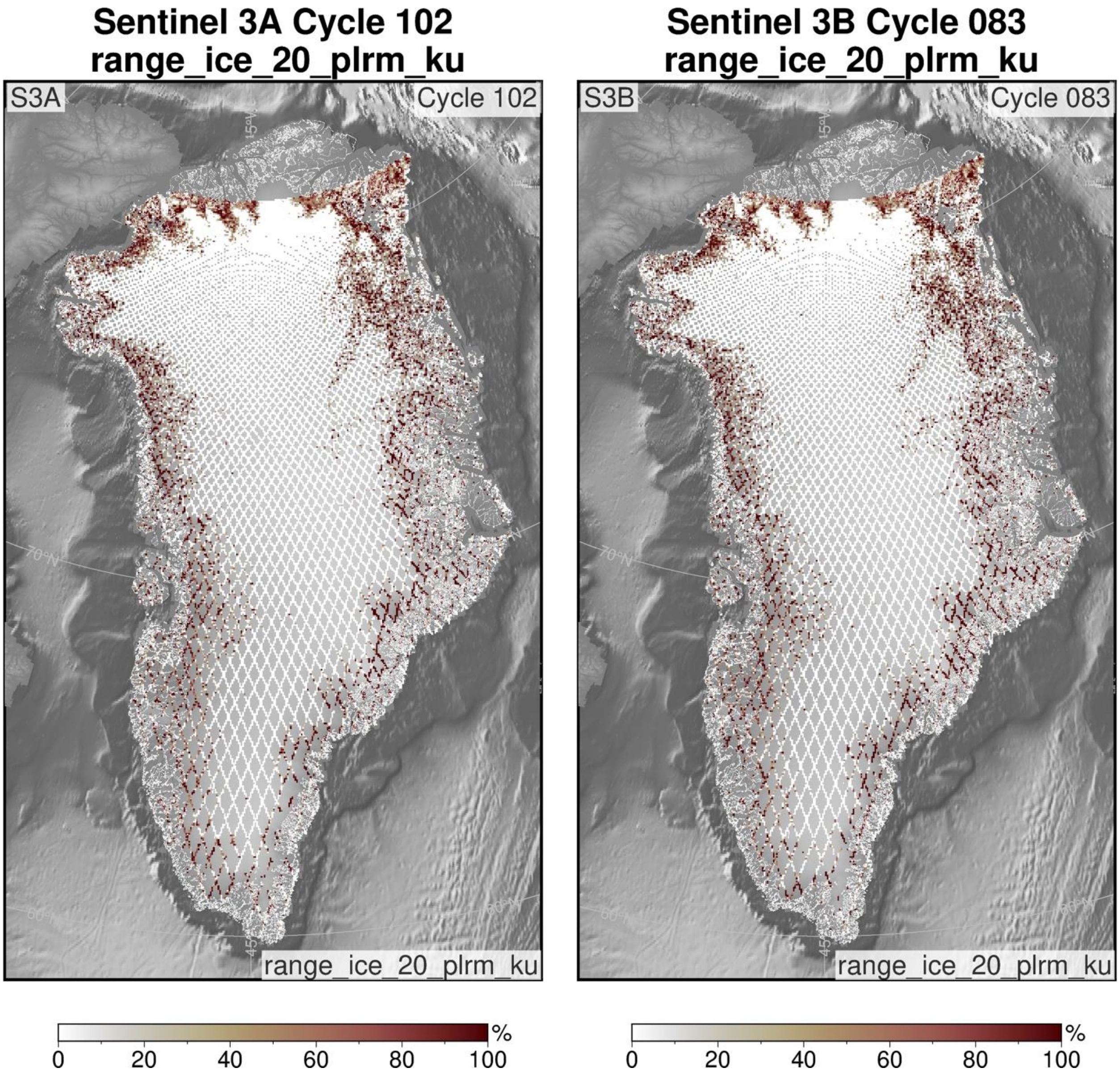

Figure 5.30 Percentage of failure over the Greenland Ice sheet for the range_ice_20_plrm_ku parameter

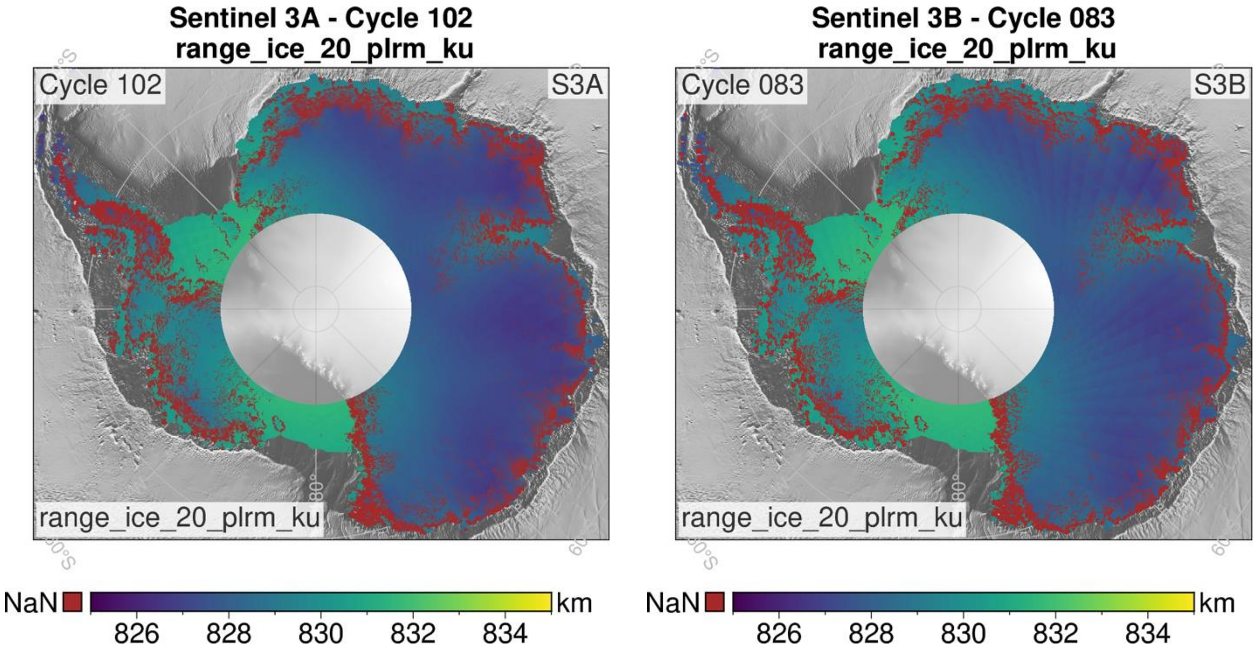

Figure 5.31 PLRM range over the Antarctica Ice sheet from the range_ice_20_plrm_ku parameter

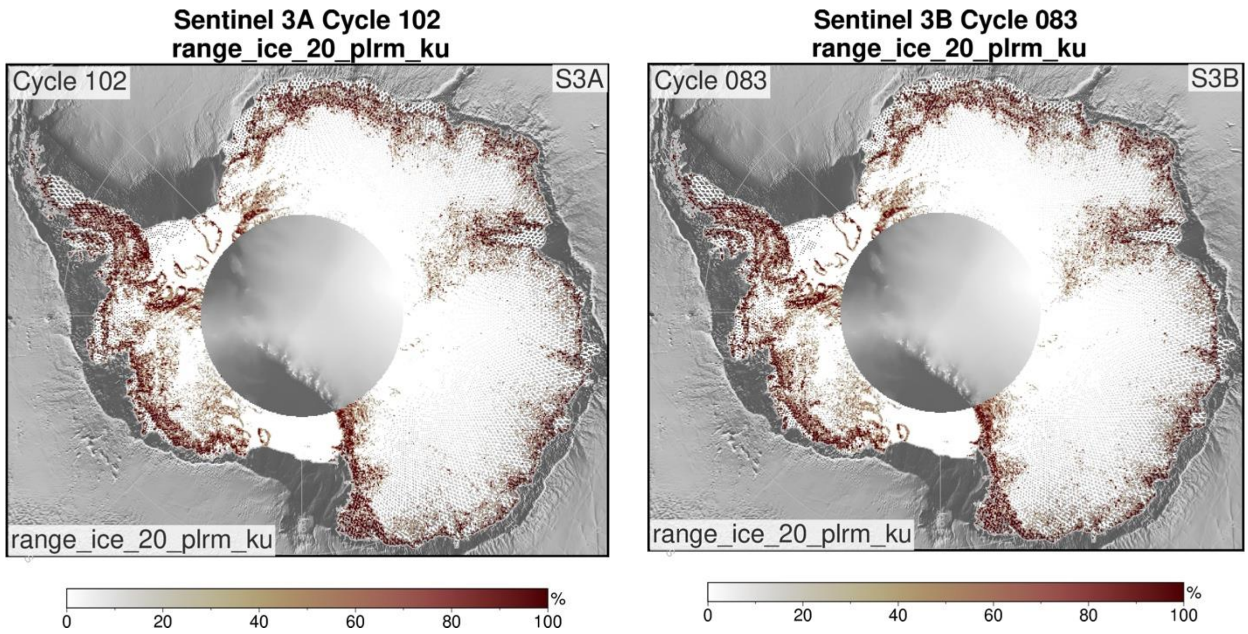

Figure 5.32 Percentage of failure over Antarctica from the range_ice_20_plrm_ku parameter

5.1.8 PLRM Ice Sigma0 (sig0_ice_20_plrm_ku)

The backscatter coefficient (sigma0) derived from the 20 Hz Ku-PLRM waveform (sig0_ice_20_plrm_ku) parameter are shown below. The PLRM Sigma0 over the Greenland and the Antarctica ice sheets are shown in Figure 5.33 and Figure 5.36, respectively. Their respective percentage of parameter failure (NaN reported) are shown in Figure 5.35 and Figure 5.38. The latter are evaluated in 5x5 km grid cells in Greenland and in 10x10 km grid cells in Antarctica.

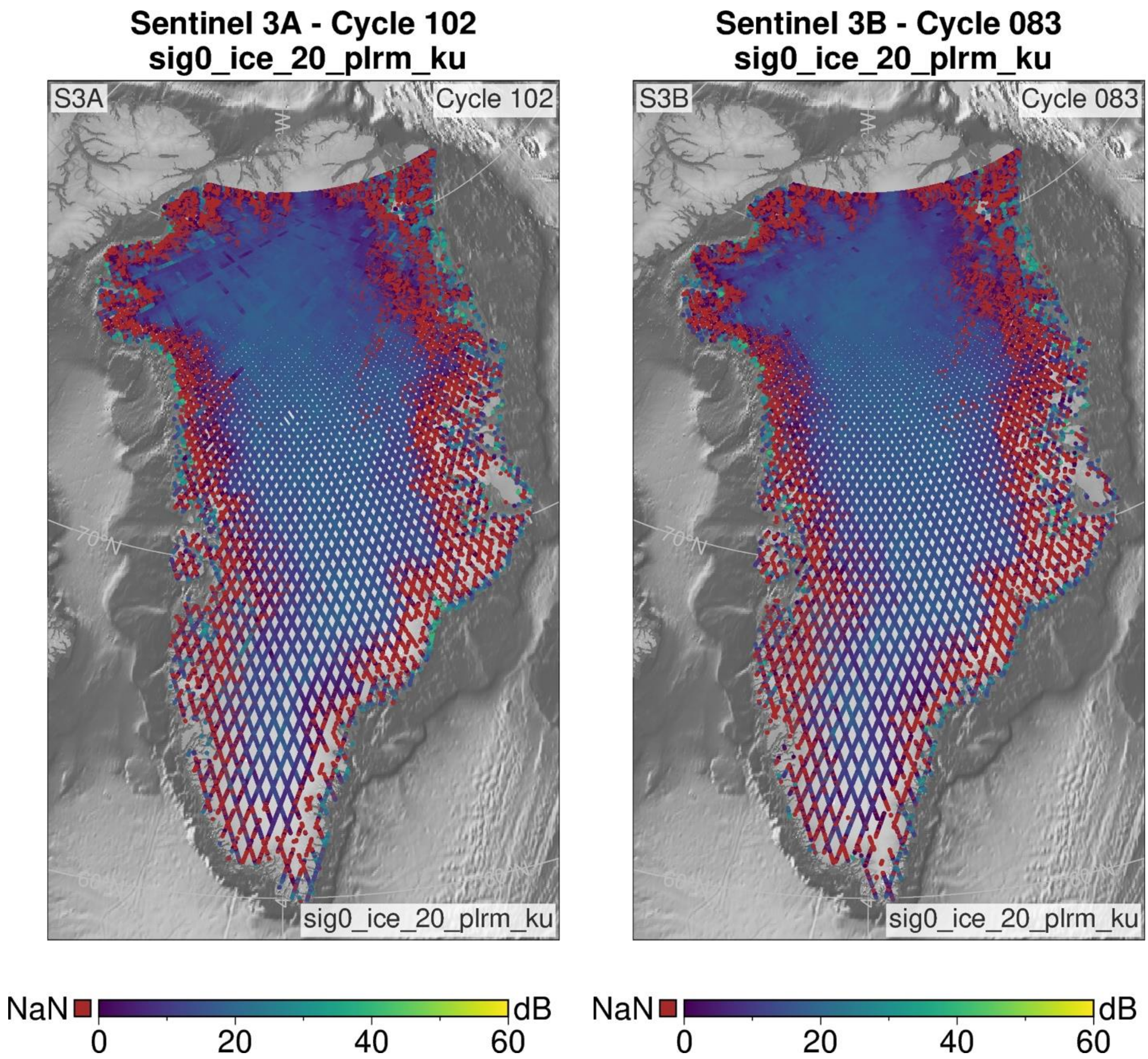

Figure 5.33 PLRM backscatter coefficient over Greenland from the sig0_ice_20_plrm_ku parameter

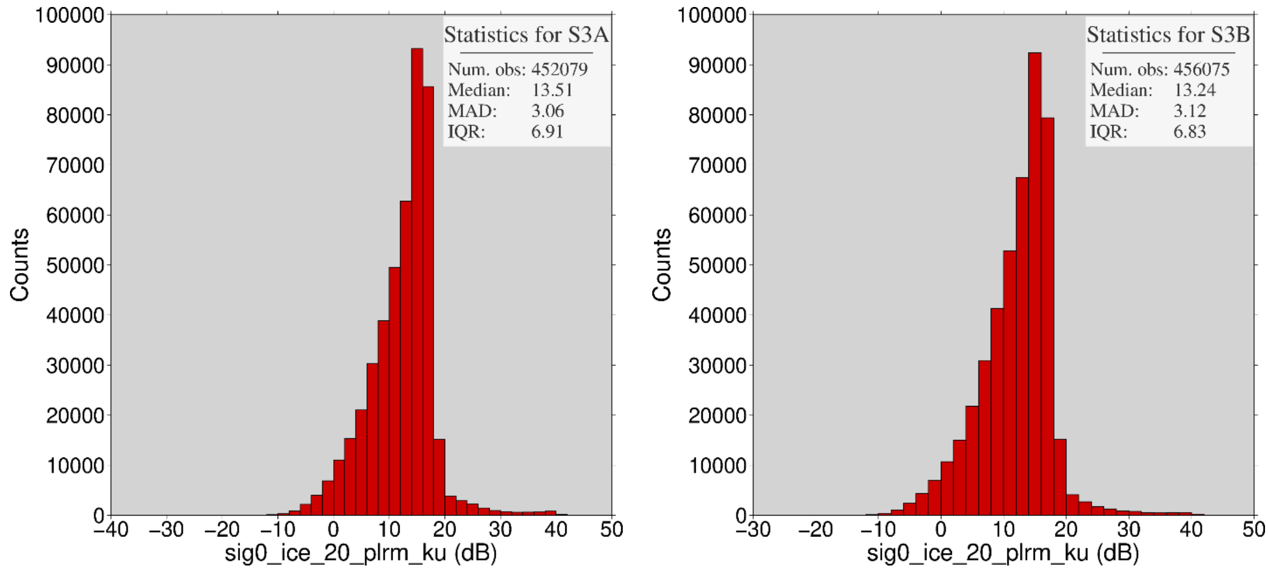

Figure 5.34 The backscatter coefficient (sig0_ice_20_plrm_ku) distribution over Greenland and statistics given by the Number of Observations, Median (dB), Median Absolute distribution (MAD) in dB, and the Interquartile Range (IQR) in dB.

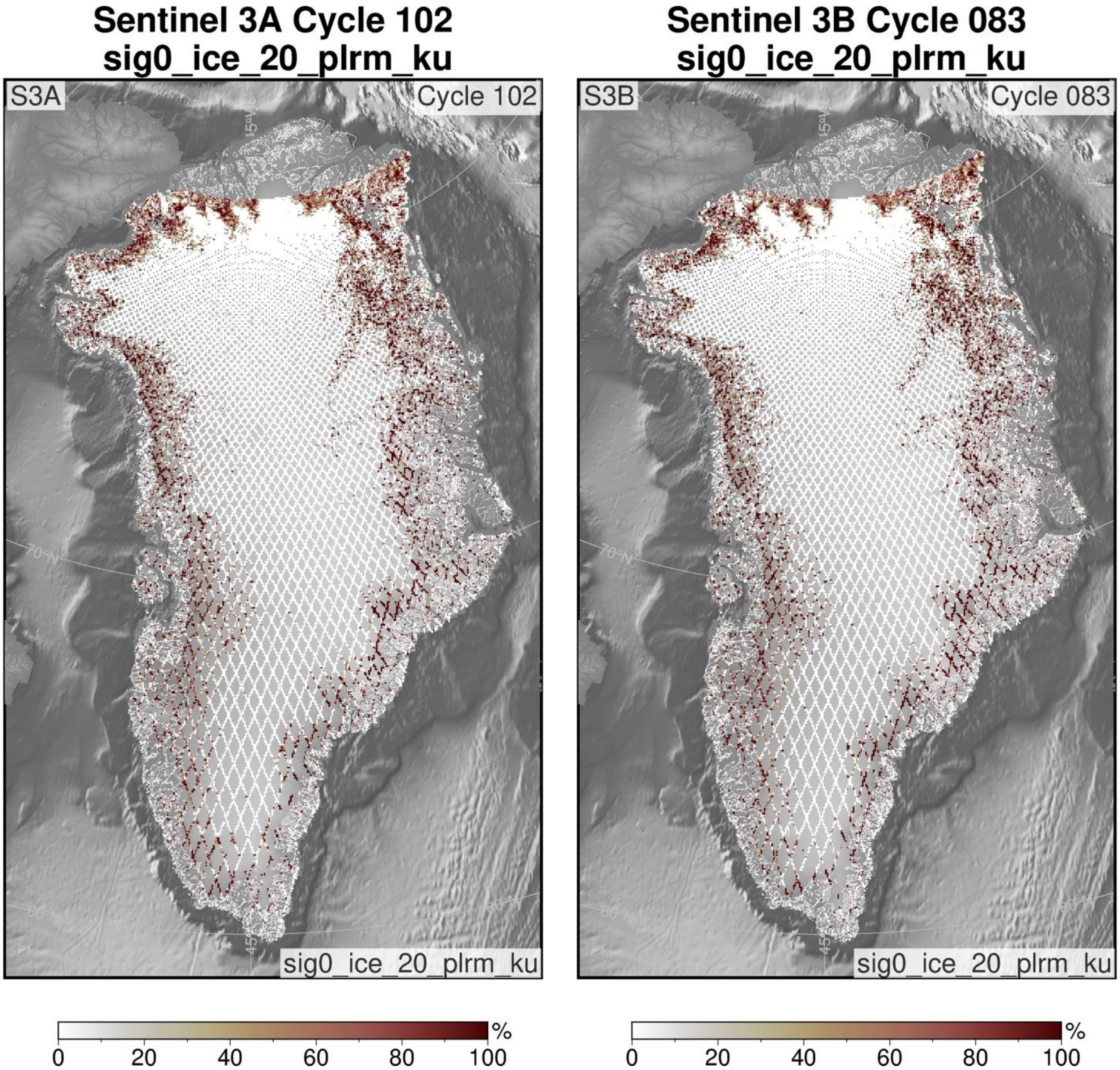

Figure 5.35 Percentage of failure over the Greenland Ice sheet from the sig0_ice_20_plrm_ku parameter

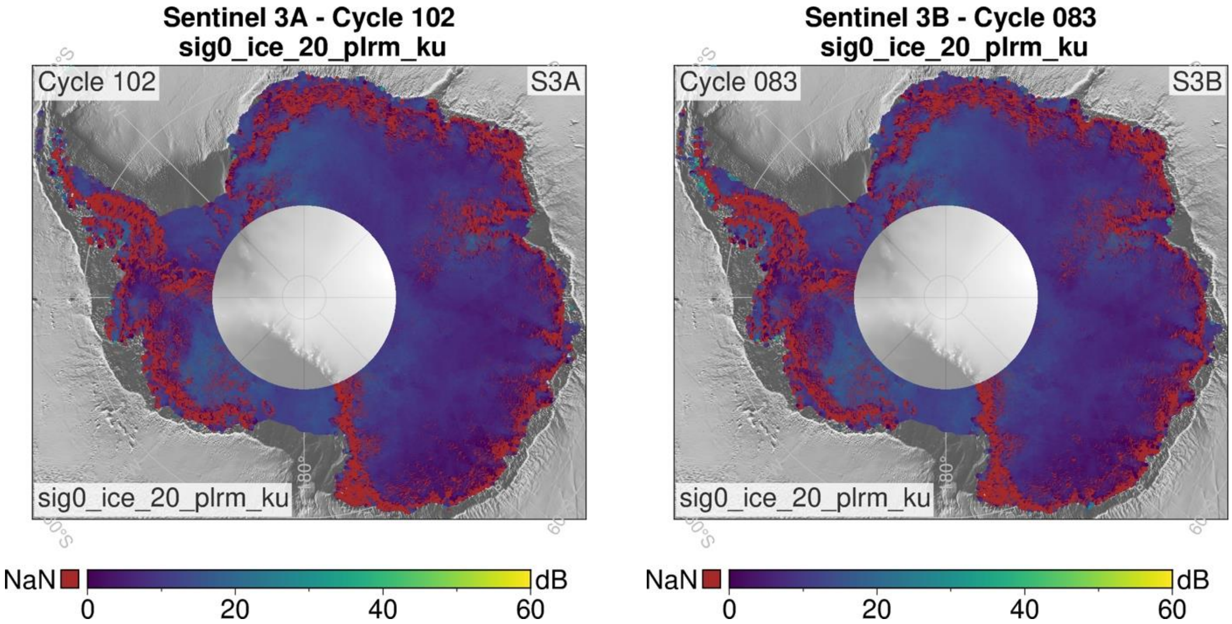

Figure 5.36 PLRM backscatter coefficient over Antarctica from the sig0_ice_20_plrm_ku parameter

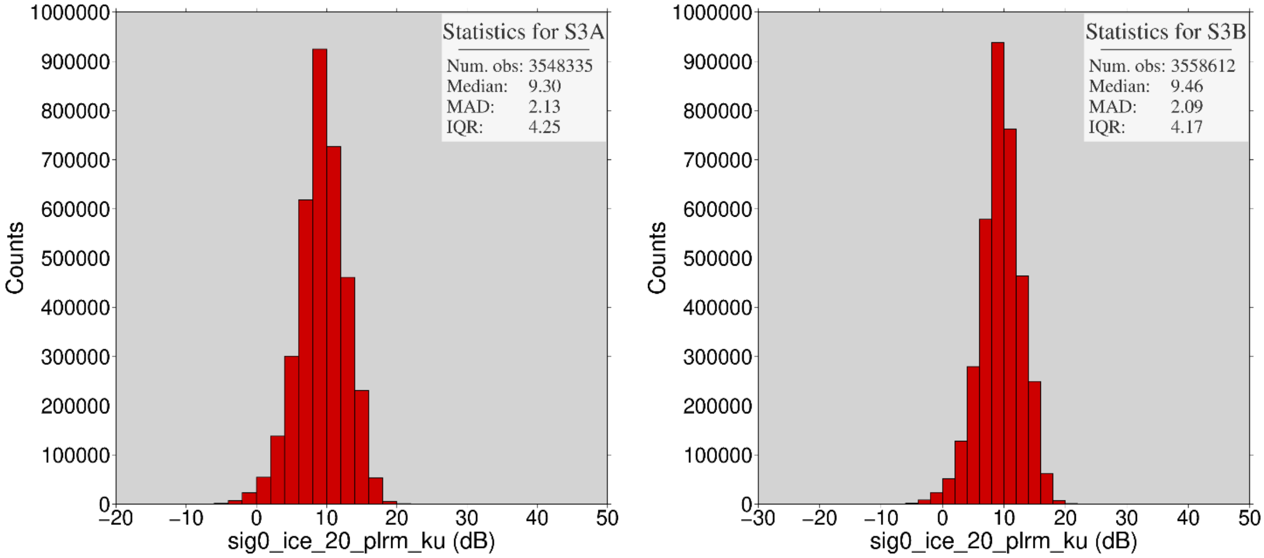

Figure 5.37 The backscatter coefficient (sig0_ice_20_plrm_ku) distribution over Antarctica and statistics given by the Number of Observations, Median (dB), Median Absolute distribution (MAD) in dB, and the Interquartile Range (IQR) given in dB.

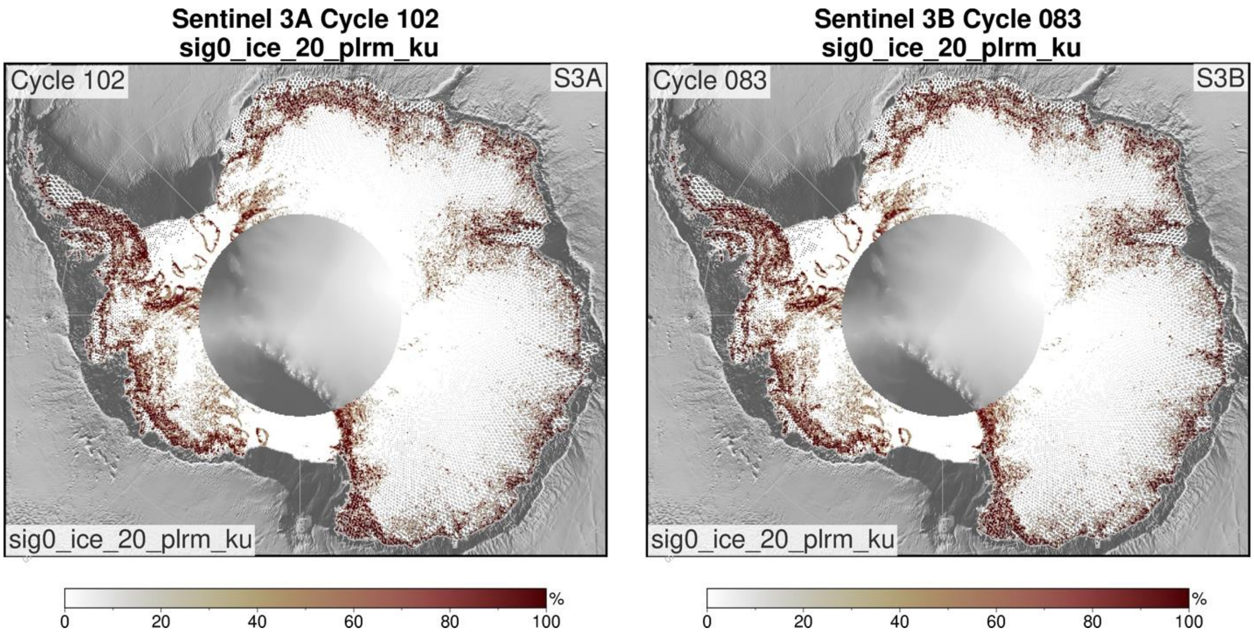

Figure 5.38 Percentage of failure over Antarctica for the sig0_ice_plrm_ku parameter

5.1.9 Waveform Quality Flag (waveform_qual_ice_20_ku)

The waveform quality flag gives the data users information about the quality of the waveforms for use in the calculation of range and elevation, and hence on the useability of the data. The criteria applied to assess each waveform are listed below Table 2.1. The value of waveform_qual_ice_20_ku is zero (ok) if all tests are passed. The waveform quality flags for the present S3A and S3B cycles are shown for the Greenland ice sheet in Figure 5.39, and for Antarctica in Figure 5.40.

Test Description	Threshold	Flag Bit Set
Total Power in waveform < threshold	2500	1
Average noise power in gates 6-9* > threshold *Noise gates starts at 0	12.5	2
Variance > threshold	7.0	4
Leading Edge Test > threshold Flag set if power to left of gate 42 > threshold * power to right	1.0	8
Peakiness < Low Threshold	0.9	16
Peakiness > High Threshold	1e12	32

Table 5.1 The thresholds used for each waveform quality test

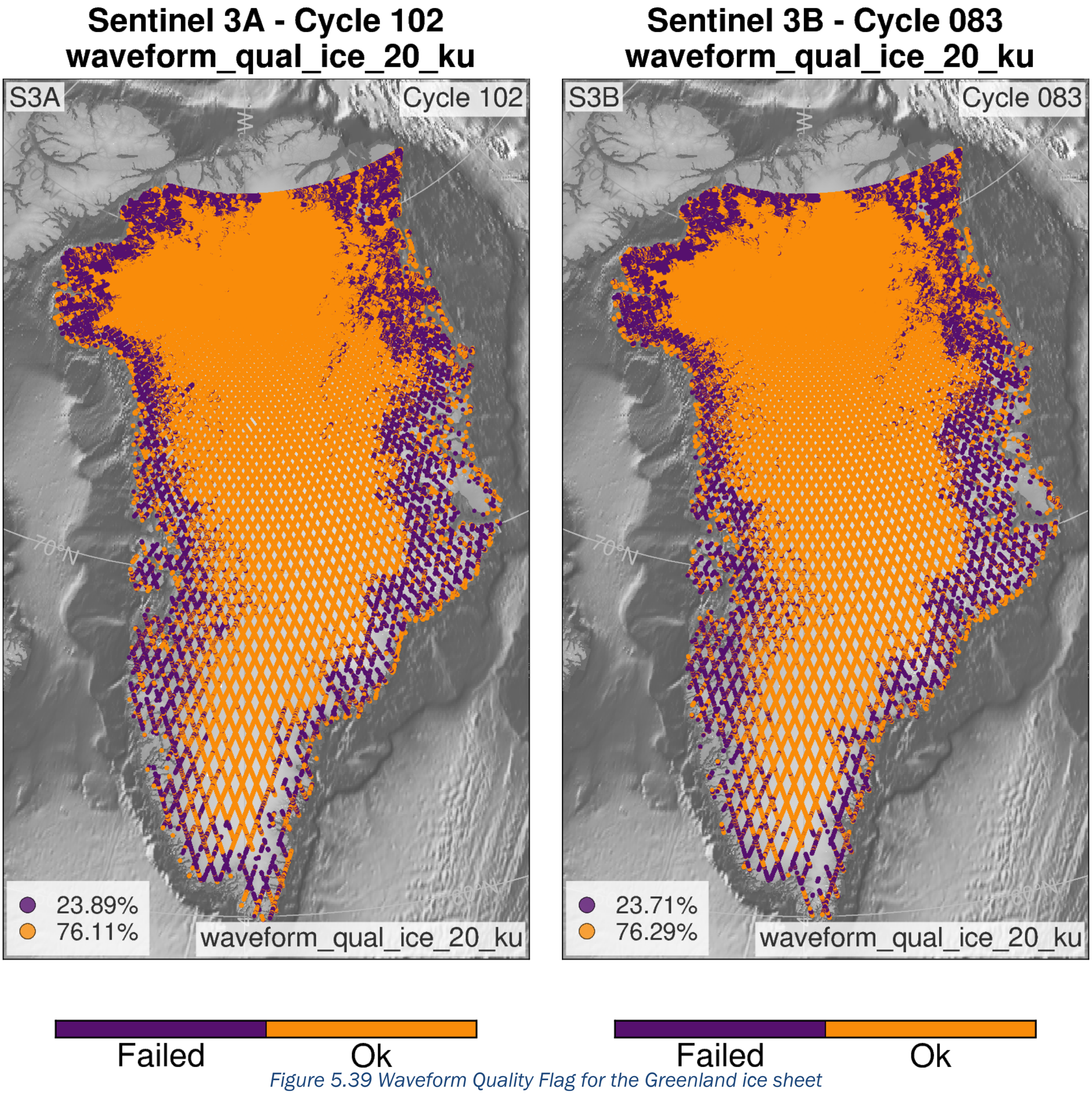

Figure 5.39 Waveform Quality Flag for the Greenland ice sheet

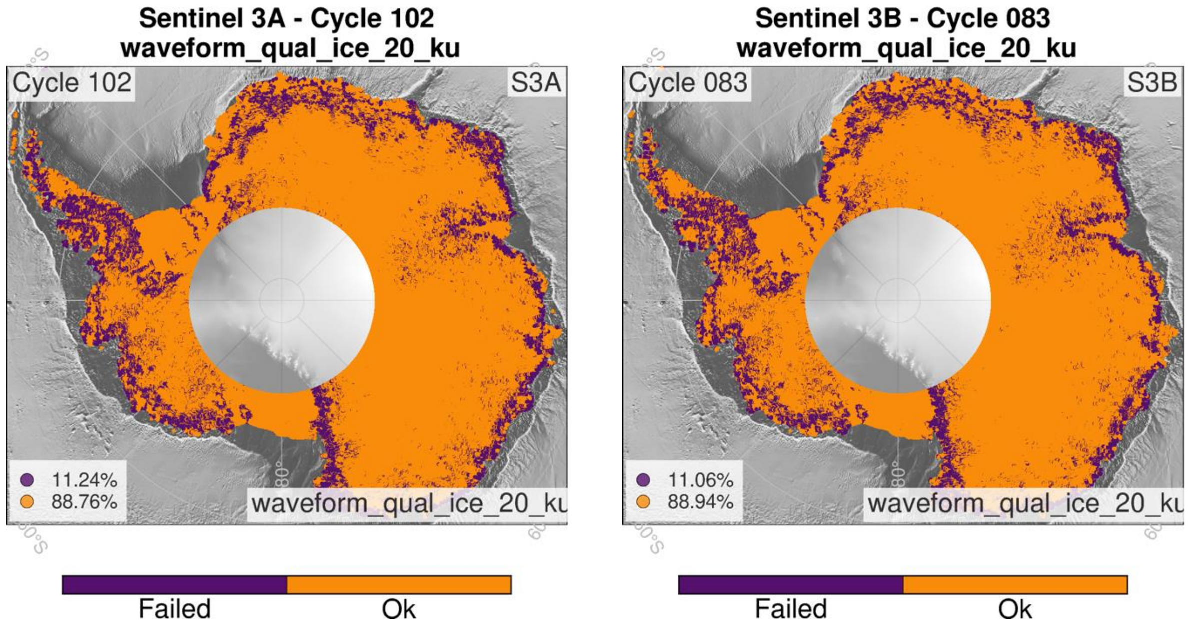

Figure 5.40 Waveform Quality Flag for Antarctica

5.1.10 Slope correction

A slope correction is applied to each measurement to relocate the SAR echo to the point of closest approach (POCA). The slope-corrected coordinates are given by the variables lat_cor_20_ku and lon_cor_20 ku for the 20 Hz Ku measurements. The figures below show whether the slope correction was successful or not over Greenland (Figure 5.41) and Antarctica (Figure 5.42).

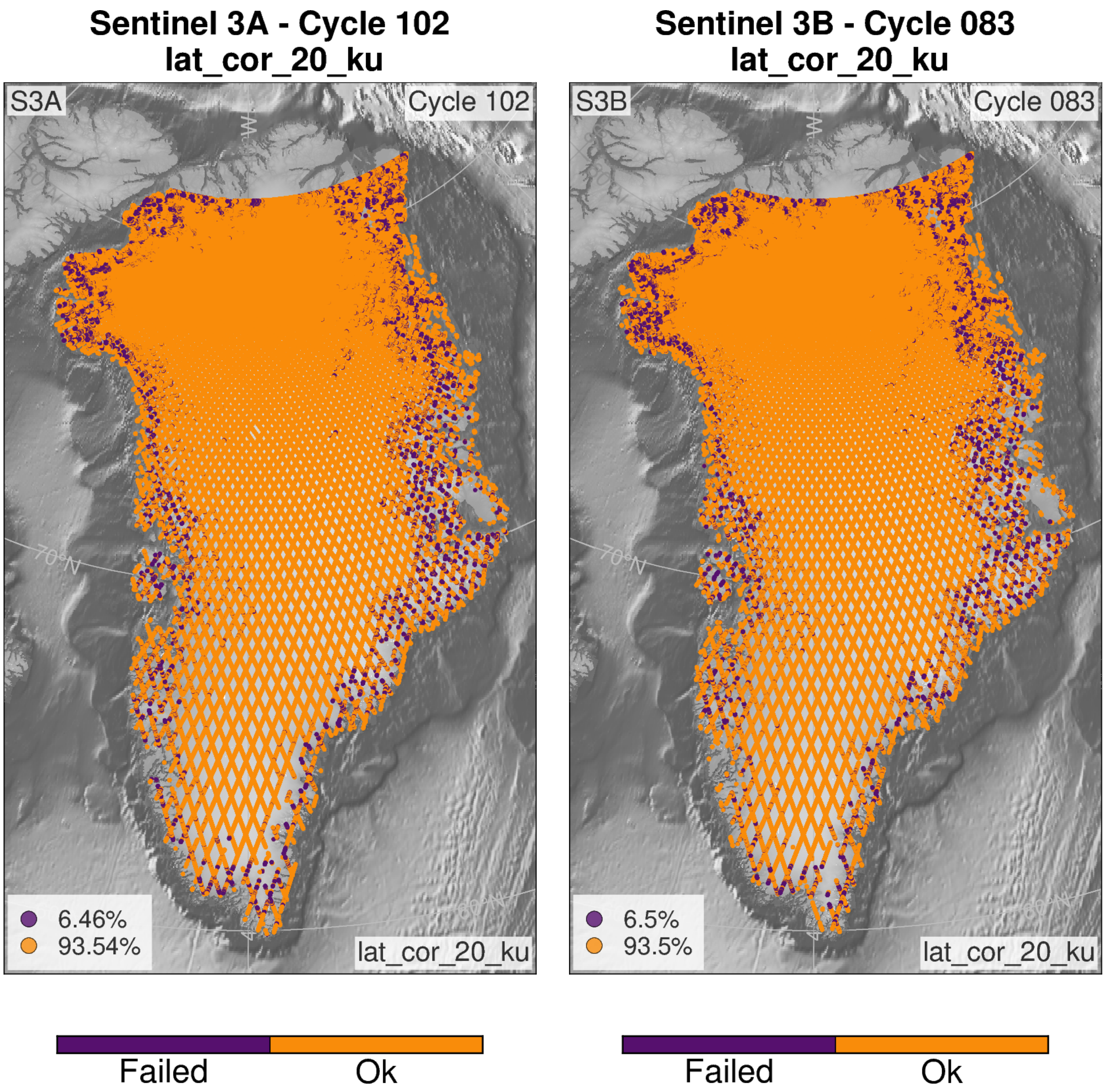

Figure 5.41 Slope correction failure for the Greenland ice sheet

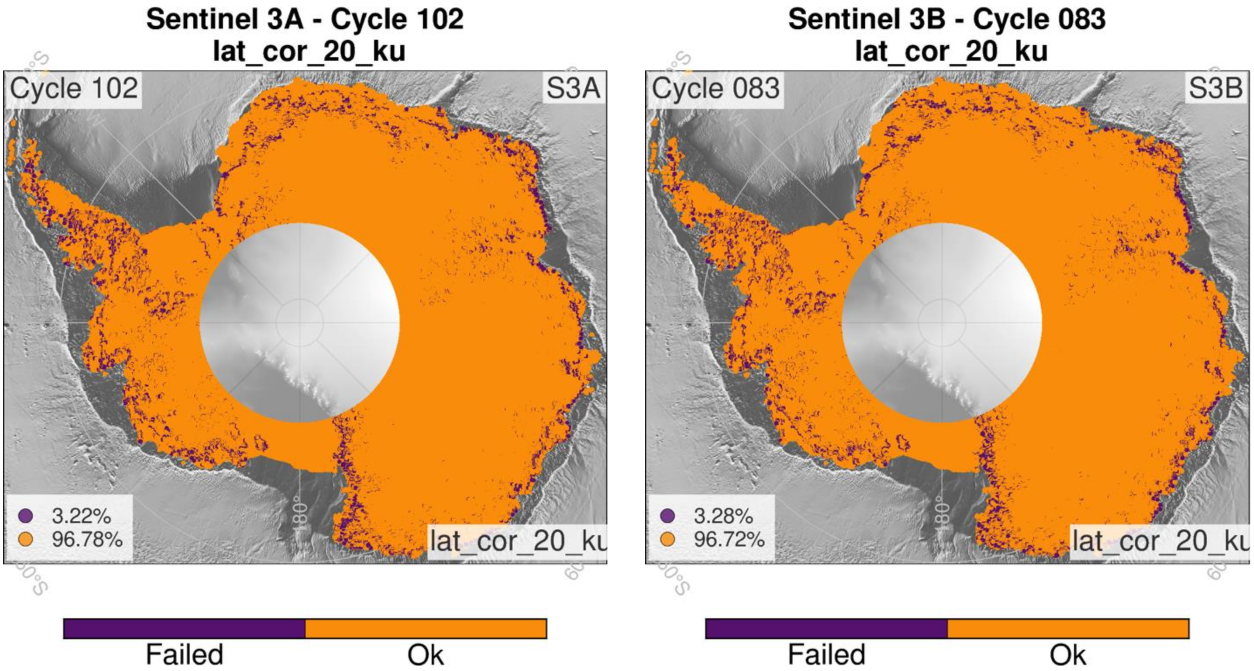

Figure 5.42 Slope correction failure for Antarctica

6 Crossover Analysis

The observed elevation difference at ground-track crosses is a primary method of assessing the precision of L2 altimetry elevation data. Here, we assess the elevation difference for the two available retrackers:

- UCL Ice sheet retracker ("elevation_ice_sheet_20_ku")
- OCOG/ICE-1 retracker (“elevation_ocog_sheet_20_ku")

The crossover difference of the elevation observations is derived for the full cycle of observations. It should be noted that the ice sheet surface elevation is in some area changing over the timespan of a cycle due to e.g., weather and snowpack properties. This may give raise to a natural crossover bias which is not associated with the precision of L2 altimetry elevation data. Therefore, for more in-depth analysis the timing between crossovers should be shortened. The crossover statistics are below as tables, maps, and histograms.

6.1 Greenland

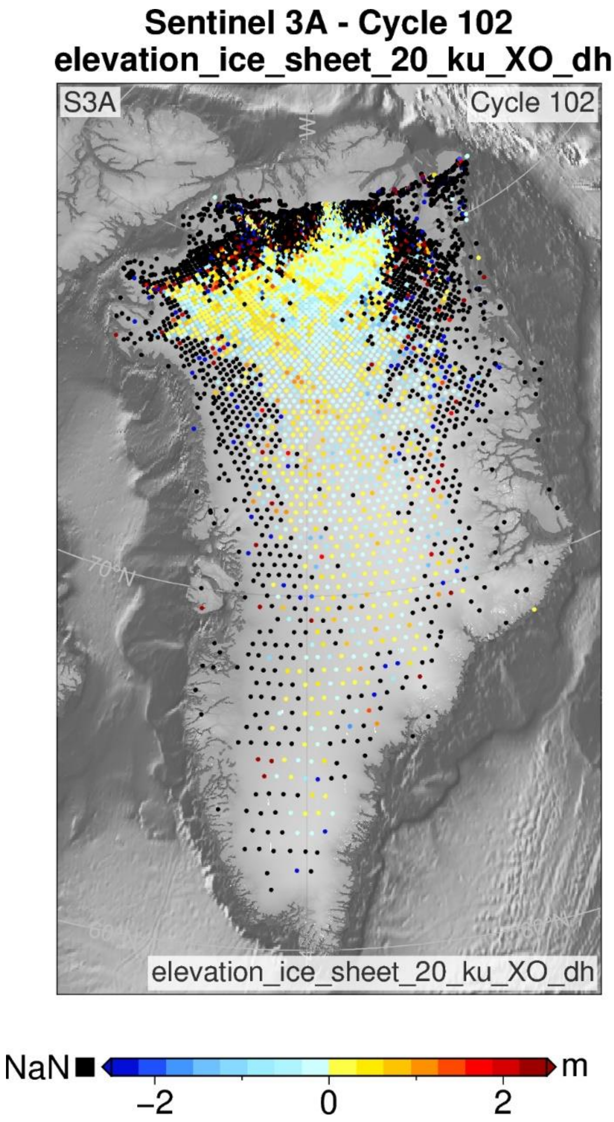

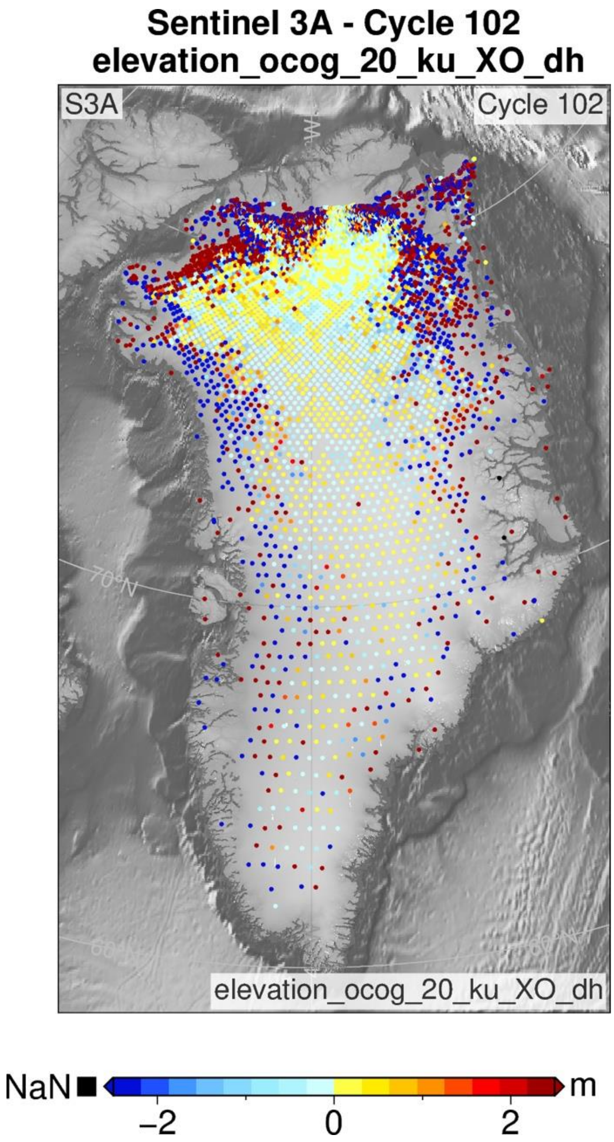

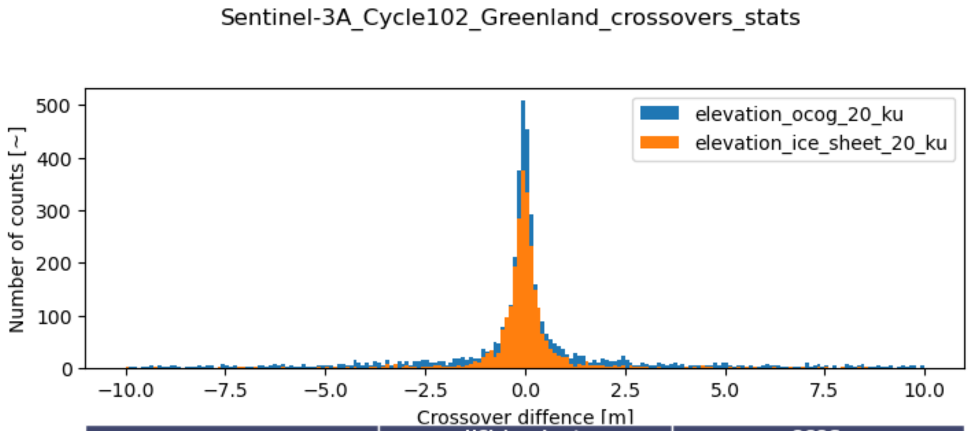

Statistics	UCL ice sheet retracker	OCOG retracker
Total number Observation [#]	2941.0	7626.0
Median [m]	-0.027	0.005
Std [m]	247.349	153.169
Observ. [%] (dh < 1 m)	78.749	37.936
Median [m] (dh < 1 m)	-0.026	-0.02
Std [m] (dh < 1 m)	0.347	0.354

Figure 6.1 SAR mode elevation differences at ground track crossover locations for Sentinel-3A, for the two retrackers (upper panel). Histograms of crossover elevation differences (lower panel)

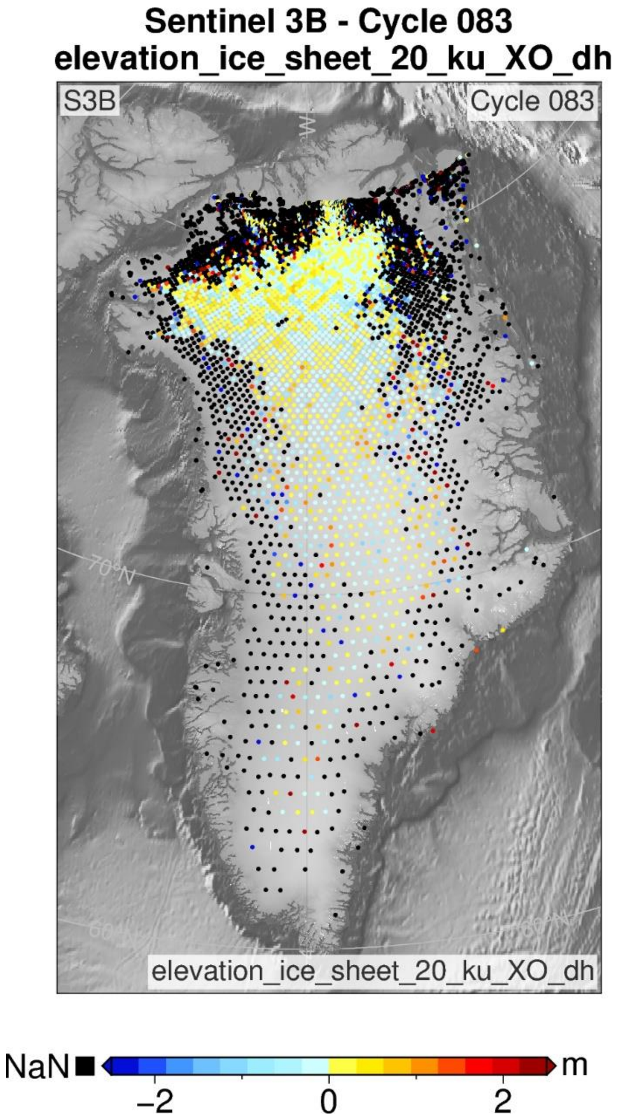
Sentinel 3B - Cycle 083
elevation_ice_sheet_20_ku_XO_dh
S3B
Cycle 083
70°N
elevation_ice_sheet_20_ku_XO_dh
NaN
m
−2
0
2

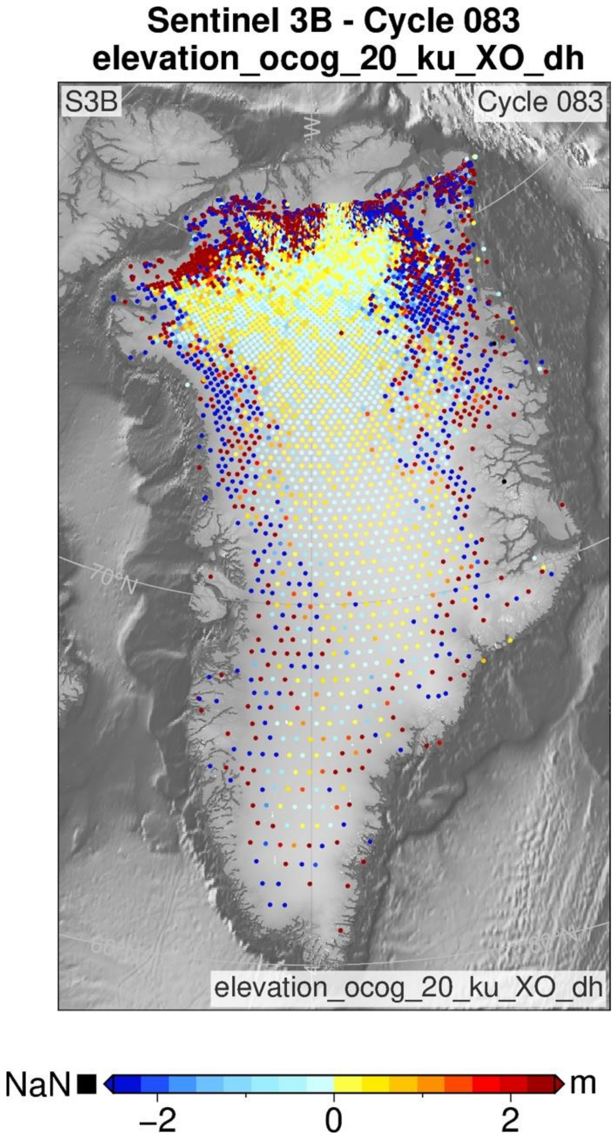
Sentinel 3B - Cycle 083
elevation_ocog_20_ku_XO_dh
S3B
Cycle 083
70°N
elevation_ocog_20_ku_XO_dh
NaN
m
−2
0
2

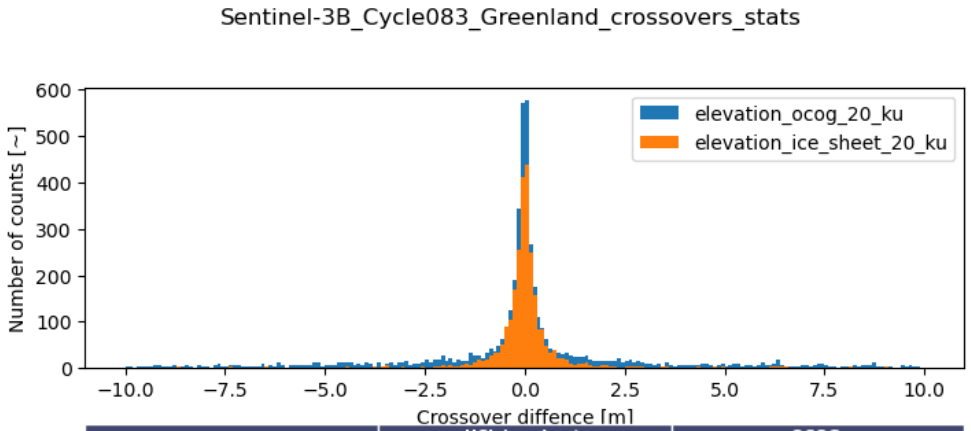

Statistics	UCL ice sheet retracker	OCOG retracker
Total number Observation [#]	2988.0	8327.0
Median [m]	-0.002	0.005
Std [m]	192.174	178.667
Observ. [%] (dh < 1 m)	78.916	35.427
Median [m] (dh < 1 m)	-0.002	-0.007
Std [m] (dh < 1 m)	0.33	0.334

Figure 6.2 SAR mode elevation differences at ground track crossovers for Sentinel-3B for the two retrackers (upper panel). Histograms of crossover elevation differences (lower panel)

6.2 Antarctica

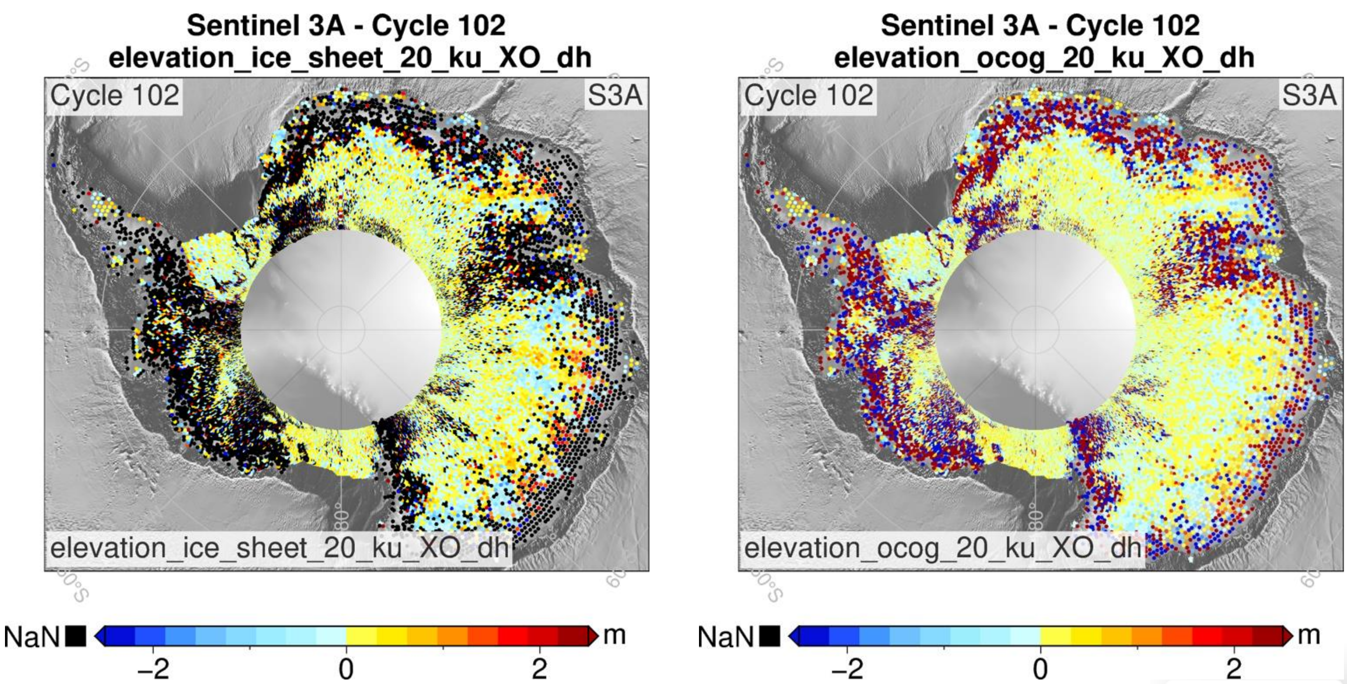

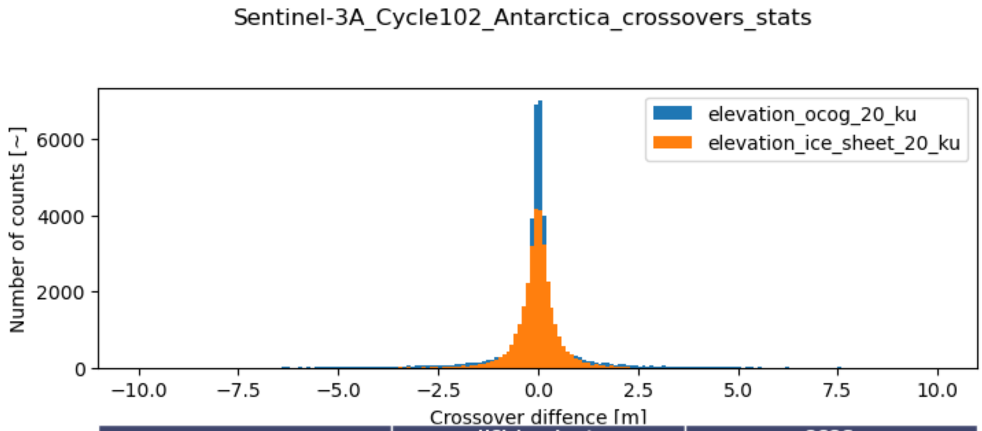

Statistics	UCL ice sheet retracker	OCOG retracker
Total number Observation [#]	34079.0	48807.0
Median [m]	-0.004	0.001
Std [m]	142.75	68.299
Observ. [%] (dh < 1 m)	87.643	72.543
Median [m] (dh < 1 m)	-0.002	0.001
Std [m] (dh < 1 m)	0.358	0.317

Figure 6.3 SAR mode elevation differences at ground track crossover locations for Sentinel-3A, for the two retrackers (upper panel). Histograms of crossover elevation differences (lower panel).

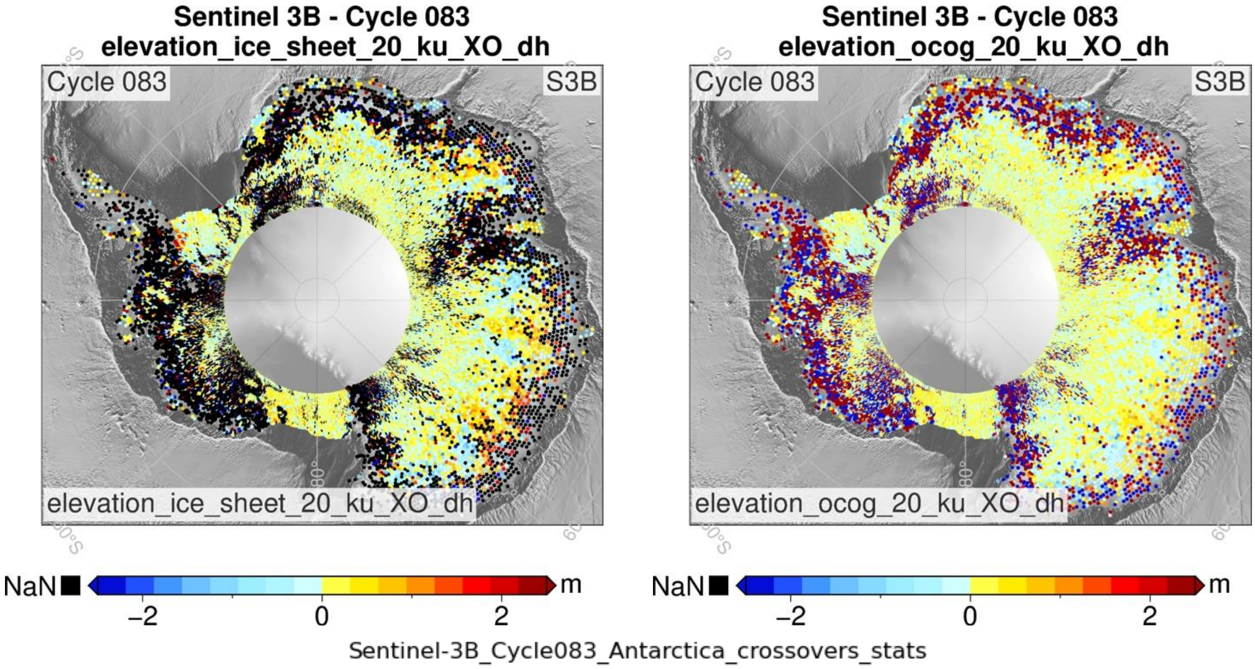

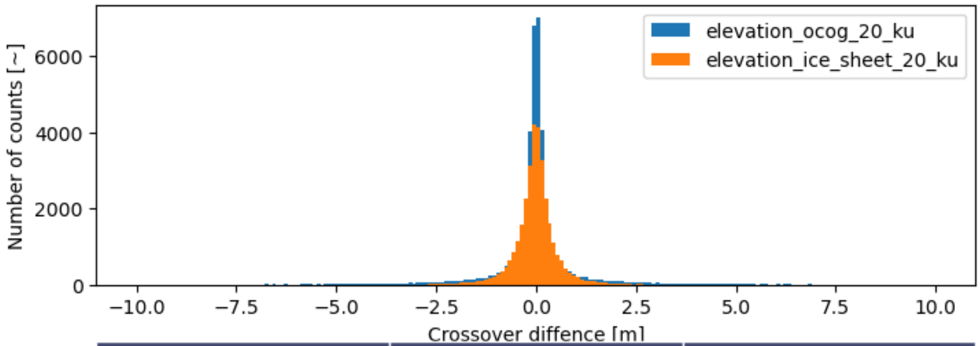

Statistics	UCL ice sheet retracker	OCOG retracker
Total number Observation [#]	34226.0	49187.0
Median [m]	-0.004	0.002
Std [m]	131.295	70.991
Observ. [%] (dh < 1 m)	87.398	72.137
Median [m] (dh < 1 m)	-0.002	0.0
Std [m] (dh < 1 m)	0.359	0.32

Figure 6.4 SAR mode elevation differences at ground track crossovers for Sentinel-3B for the two retrackers (upper panel). Histograms of crossover elevation differences (lower panel)

Appendix A - Useful links

The Product Format Specification applicable to the SRAL Level 2 products assessed in this report is available in Sentinel Online, version 2.15:

https://sentinel.esa.int/documents/247904/2753172/Sentinel-3-Product-Data-Format-Specification-Level-2-Land.pdf/a176f07a-d9bd-4589-8c29-92c3487a9c7b?t=1611592513420

All cyclic performance reports are available on the mission performance cluster page at Sentinel-online webpage:

https://sentinel.esa.int/web/sentinel/technical-guides/sentinel-3-altimetry/mission-performance

All plots were made using Python and PyGMT (0.8.0) a Python wrapper for The Generic Mapping Tools (GMT) Version 6.3.0 (Wessel et al. 2019; Uieda et al. 2021)

Appendix B - References

Bamber, J. L. 1994. "Ice Sheet Altimeter Processing Scheme." *International Journal of Remote Sensing* 15 (4): 925–38. https://doi.org/10.1080/01431169408954125.

Legresy, Benolt, and Frede Rique Remy. 1997. "Altimetric Observations of Surface Characteristics of the Antarctic Ice Sheet." *Journal of Glaciology* 43 (144): 265275.

Uieda, Leonardo, Dongdong Tian, Wei Ji Leong, Meghan Jones, William Schlitzer, Liam Toney, Michael Grund, et al. 2021. "PyGMT: A Python Interface for the Generic Mapping Tools," October. https://doi.org/10.5281/ZENODO.5607255.

Wessel, P., J. F. Luis, L. Uieda, R. Scharroo, F. Wobbe, W. H.F. Smith, and D. Tian. 2019. "The Generic Mapping Tools Version 6." *Geochemistry, Geophysics, Geosystems* 20 (11). https://doi.org/10.1029/2019GC008515.

Wingham D J, Rapley C G, and Griffiths H. 1986. "New Techniques in Satellite Altimeter Tracking Systems." In , 1339–44. Proc. IGARSS'86 Symposium.

Wingham, D. J., and D. W. Wallis. 2010. "The Rough Surface Impulse Response of a Pulse-Limited Altimeter With an Elliptical Antenna Pattern." *IEEE Antennas and Wireless Propagation Letters* 9: 232–35. https://doi.org/10.1109/LAWP.2010.2046471.